Andean Geology 39 (2): 317-357. May, 2012
doi: 10.5027/andgeoV39n2-a07

Andean Geology
formerly Revista Geológica de Chile
www.andeangeology.cl

Cenozoic structural evolution of the Argentinean Andes at 34º40'S: A close relationship between thick and thin-skinned deformation

Martín Turienzo[1], Luis Dimieri[1], Cristina Frisicale[1], Vanesa Araujo[1], Natalia Sánchez[1]

[1] *INGEOSUR-CONICET. Departamento de Geología, Universidad Nacional del Sur, San Juan 670 (8000), Bahía Blanca, Argentina. turienzo@uns.edu.ar; ldimieri@uns.edu.ar; cfrisica@uns.edu.ar; vanesa.araujo@uns.edu.ar; natalia.sanchez@uns.edu.ar*

ABSTRACT. In the Argentinean side of the Andes at 34°40'S, the Cenozoic Andean orogeny produced the thick-skinned Malargüe fold-and-thrust belt and the easternmost basement uplift of the Cordillera Frontal. Integrating balanced structural cross-sections with previous studies of Cenozoic synorogenic rocks and $^{40}Ar/^{39}Ar$ ages of coeval volcanic and subvolcanic rocks, we propose a Miocene to Quaternary sequential structural evolution of this sector of the Andes. Andean deformation in the study area begun around 14.5 Ma with the growth of thick-skinned structures at the western region, formed by large basement wedges that propagated along detachment horizons within the cover generating thin-skinned structures. The development of these genetically linked thick and thin-skinned structures finished with the insertion of a third basement wedge and its associated deformation in cover rocks along the Sosneado thrust, before the extrusion of 10.8 Ma volcanic rocks. These structures imply ~10 km of shortening, representing an important Middle Miocene compressive period (2.7 mm/a). Systems of fractures measured in basement, cover and subvolcanic rocks indicate an E-W direction of compression. A supercritical Coulomb wedge attained after the Middle Miocene deformation, was responsible of new basement-involved faulting into the foreland, the west-dipping Carrizalito thrust. The absence of efficient detachment levels in the cover rocks of the eastern region difficulted the development of large basement wedges and instead important backthrusting occurred in the hangingwall of the Carrizalito thrust. Widespread subvolcanic rocks (10.5 to 5.5 Ma) exposed in this region suggest a close relationship between magmatism and antithetic faulting. With continuing compression, the Carrizalito thrust breaks through to the surface thrusting pre-Jurassic and Mesozoic sequences over Cenozoic rocks although in the southern region it remains as a blind thrust. This different configuration along the strike of the Carrizalito thrust is due to an ENE trending oblique fault. Thick-skinned structures in the eastern sector, that involve ~4 km of shortening, were covered discordantly by horizontal basalts of ~0.5 Ma. A shortening rate of 0.42 mm/a from Late Miocene to Middle Pleistocene indicates that Andean contraction diminished, which is in agreement with most geodynamic models of plate tectonics.

Keywords: Andean tectonic, Structural evolution, Thick and thin-skinned deformation, Argentinean Andes.

RESUMEN. Evolución estructural Cenozoica de los Andes Argentinos a los 34°40'S: una estrecha relación entre deformación de piel fina y piel gruesa. En los Andes Argentinos a los 34°40'S, la orogenia Andina produjo durante el Cenozoico la faja corrida y plegada de Malargüe, de piel gruesa, y hacia el este el levantamiento del basamento en la Cordillera Frontal. Integrando secciones estructurales balanceadas con estudios previos de rocas sinorogénicas terciarias y edades $^{40}Ar/^{39}Ar$ de rocas volcánicas y subvolcánicas contemporáneas, proponemos una evolución estructural secuencial desde el Mioceno al Cuaternario para este sector de los Andes. La deformación andina en el área de estudio comenzó alrededor de los 14,5 Ma con el desarrollo de estructuras de piel gruesa en la región occidental, formadas por grandes cuñas de basamento que se propagaron a lo largo de despegues dentro de la cubierta sedimentaria, generando estructuras de piel fina. El desarrollo de esas estructuras de piel gruesa y piel fina finalizó con la inserción de una tercera cuña de basamento y su deformación asociada en la cubierta a lo largo del corrimiento Sosneado, antes de la extrusión de rocas volcánicas de 10,8 Ma. Estas estructuras implican ~10 km de acortamiento, representando un importante evento compresivo en el Mioceno Medio (2,7 mm/a). Los sistemas de fracturas medidos en el basamento, la cubierta y en rocas subvolcánicas, indican una dirección de compresión E-W. Un estado de cuña de Coulomb supercrítica alcanzado luego de la deformación del Mioceno Medio generó nuevo fallamiento en el antepaís, el corrimiento Carrizalito. La ausencia de niveles de despegue eficientes en las rocas de la cubierta en la región oriental dificultó el desarrollo de grandes cuñas de basamento y en cambio tuvo lugar una importante deformación mediante retrocorrimientos en el bloque colgante del corrimiento Carrizalito. La abundante presencia de rocas subvolcánicas (10,5 a 5,5 Ma) en la región de retrocorrimientos sugiere que existe una estrecha relación entre el magmatismo y dicho fallamiento antitético. Con la continuidad de la compresión el corrimiento Carrizalito cortó hacia la superficie sobrecorriendo a las secuencias prejurásicas y mesozoicas sobre rocas terciarias, aunque al sur permanece como un corrimiento ciego. Este diferente desplazamiento a lo largo del rumbo del corrimiento Carrizalito se acomoda mediante una falla oblicua, de rumbo ENE. Las estructuras de piel gruesa en el sector oriental, que involucran ~4 km de acortamiento, fueron cubiertas discordantemente por basaltos horizontales de ~0,5 Ma. Una tasa de acortamiento de 0,42 mm/a desde el Mioceno tardío al Pleistoceno medio indica una disminución en la contracción andina, lo cual concuerda con la mayoría de los modelos geodinámicos de la tectónica de placas.

Palabras clave: Tectónica andina, Evolución estructural, Deformación de piel gruesa y piel fina, Andes Argentinos.

1. Introduction

Understanding the development through time of the structures that constitute a fold and thrust belt is decidedly important to comprehend the tectonic evolution of any orogenic belt worldwide. Diverse geological information must be considered in order to analyze the kinematics of a fold and thrust belt, including age, composition and distribution of synorogenic sediments; absolute ages of igneous rocks formed before, during and after the different deformation pulses; and the geometry of the main structures both in surface and in depth. The Malargüe fold-and-thrust belt (Malargüe FTB), which forms part of the Cordillera Principal in the Andes of central western Argentina (Fig. 1), is a thick-skinned belt developed during the Cenozoic Andean orogeny that offers an exceptional opportunity to understand its structural architecture and evolution because of the extremely good exposures and the abundance of geological and geophysical data. Our studies were developed in the region between the Río Diamante and Río Atuel (34°30'-34°50'S), in the west of Mendoza province, where the Mesozoic units of the Malargüe FTB overlay the pre-Jurassic basement rocks that crop out in the Cordón del Carrizalito at the southern part of the Cordillera Frontal (Figs. 1b and 1c). The geometry of basement-involved structures and its relationship with cover rocks is easily recognized because they are notably well-exposed along the Río Diamante canyon. This in turn helps us identify and comprehend the thick-skinned structures of other sectors where outcrops of basement rocks are absent or scarce. Large amounts of synorogenic Neogene sediments were accumulated intimately associated with the Andean mountain building, although in the studied area they are only partially preserved in the mountain front (Kozlowski, 1984; Yrigoyen, 1993; Combina *et al*., 1993; Combina and Nullo, 1997, 2000, 2005, 2008, 2011). A profuse Cenozoic magmatic activity produced widespread volcanic and subvolcanic rocks, whose absolute ages were established by $^{40}Ar/^{39}Ar$ dating (Baldauf *et al*., 1992; Baldauf, 1997, Giambiagi *et al*., 2008).

The main goal of this work is to propose a kinematic model in order to explain the structural

evolution of this segment of the Malargüe FTB and the Cordillera Frontal produced by the Andean orogeny, and to consider the role of thick and thin-skinned structures during the Neogene mountain building. Furthermore, we focus our study in the relationship between the tectonic structures and the Cenozoic igneous and sedimentary rocks. Balanced structural cross-sections allow us to characterize the structural style in this portion of the Andes, to evaluate the variations along strike of the major structures and to calculate the tectonic shortenings. The fracture pattern recognized in basement, cover and Cenozoic subvolcanic rocks in the entire studied area unveils the direction of tectonic compression responsible of the major structures. The sequential reconstruction of the structures leads to the distinction of two major periods of compressive deformation with its respective shortening rates (mm/a). In this way, our kinematic reconstruction suggests a period of maximum contraction during the Middle Miocene that diminished considerably in the Late Miocene-Pleistocene, which is consistent with predictions from geodetic models (Norabuena *et al*., 1999; Kendrik *et al*., 2003) and regional studies of plate dynamics (Pardo Casas and Molnar, 1987; Somoza, 1998) that reveal a decreasing convergence rate between the Nazca and South American plates.

2. Tectonic framework

The Andes is the most important subduction-related mountain chain (Dewey and Bird, 1970; James, 1971) formed along the western side of South America due to the subduction of the oceanic Nazca plate beneath the South American continental margin (Fig. 1a). A variety of tectonic, magmatic and accretionary processes occurred since the Paleozoic to recent times giving birth to the heterogeneous geological configuration that characterize the central-west side of Argentina (Ramos, 1988, 2009). Intense Late Paleozoic-Triassic magmatism related to subduction at the southwestern side of Gondwana produced granitoids and widespread volcanic rocks, mostly located in the Cordillera de la Costa (Hervé *et al.*, 1981) and Cordillera Frontal (Llambías *et al*., 1993) (Fig. 1b). Generalized extension during the Triassic formed numerous narrow and elongate depressions oriented NW-SE near the Proto-Pacific margin of Southwest Gondwana (Charrier, 1979; Uliana *et al*., 1989; Ramos and Kay, 1991; Spalletti, 1999). In the provinces of Neuquén and Mendoza, Late Triassic-Early Jurassic rifting originated the initial depocenters of the Neuquén Basin (Legarreta and Gulisano, 1989; Franzese and Spalletti, 2001), one of the most important hydrocarbon-producing sedimentary basins in Argentina (Fig. 1b). From Middle Jurassic to Early Cretaceous, accumulation of sediments in the Neuquén basin was mainly controlled by thermal subsidence in a back-arc setting, where relative changes in the sea level produced alternating deposition of marine and continental sediments (Legarreta and Gulisano, 1989; Legarreta and Uliana, 1991). Despite that is uncertain when the compressive deformation start, sedimentological evidences support the development of a foreland basin at the end of the Cretaceous possibly produced by tectonic loading related to an incipient thrust belt (Ramos, 1988; Ramos and Folguera, 2005; Tunik *et al*., 2010).

The Cenozoic Andean compression deformed all these materials (Paleozoic to Triassic igneous and Mesozoic sedimentary rocks of the Neuquén basin) forming the Cordillera Principal geological province, which is divided in several fold-and-thrust belts along its strike (Fig. 1b). There is consensus that the main compressive deformation in the Cordillera Principal was initiated in the Early-Middle Miocene, coeval with a thick synorogenic sequence accumulated in the foreland (Charrier and Vicente, 1972; Ramos, 1988). The geology and evolution of the Andean mountain belt at distinct latitudes is highly variable and is considered to be controlled by the convergence obliquity and the dip of the subducted Nazca plate, among other reasons (Barazangi and Isacks, 1976; Jordan *et al*., 1983; Cahill and Isacks, 1992; Ramos, 1988, 2009). Over the flat subduction segment in the Southern Central Andes, north of 33°S (Fig. 1b), there was not significant Neogene-Quaternary arc magmatism in the Argentinean side of the Andes and the deformation extended further to the east uplifting the basement blocks of the Sierras Pampeanas (Jordan *et al*., 1983; Ramos, 1988; Ramos *et al*., 2002). On the other hand over the normal subduction segment, south of 34°S, high volcanoes along the Argentina-Chile limit represent an important magmatic arc and the approximately N-S eastern mountain front is located in the Andes foothills between 69°W and 70°W. In the Chilean side of the Andes, Miocene-Pliocene magmatism produced widespread volcanic and plutonic rocks

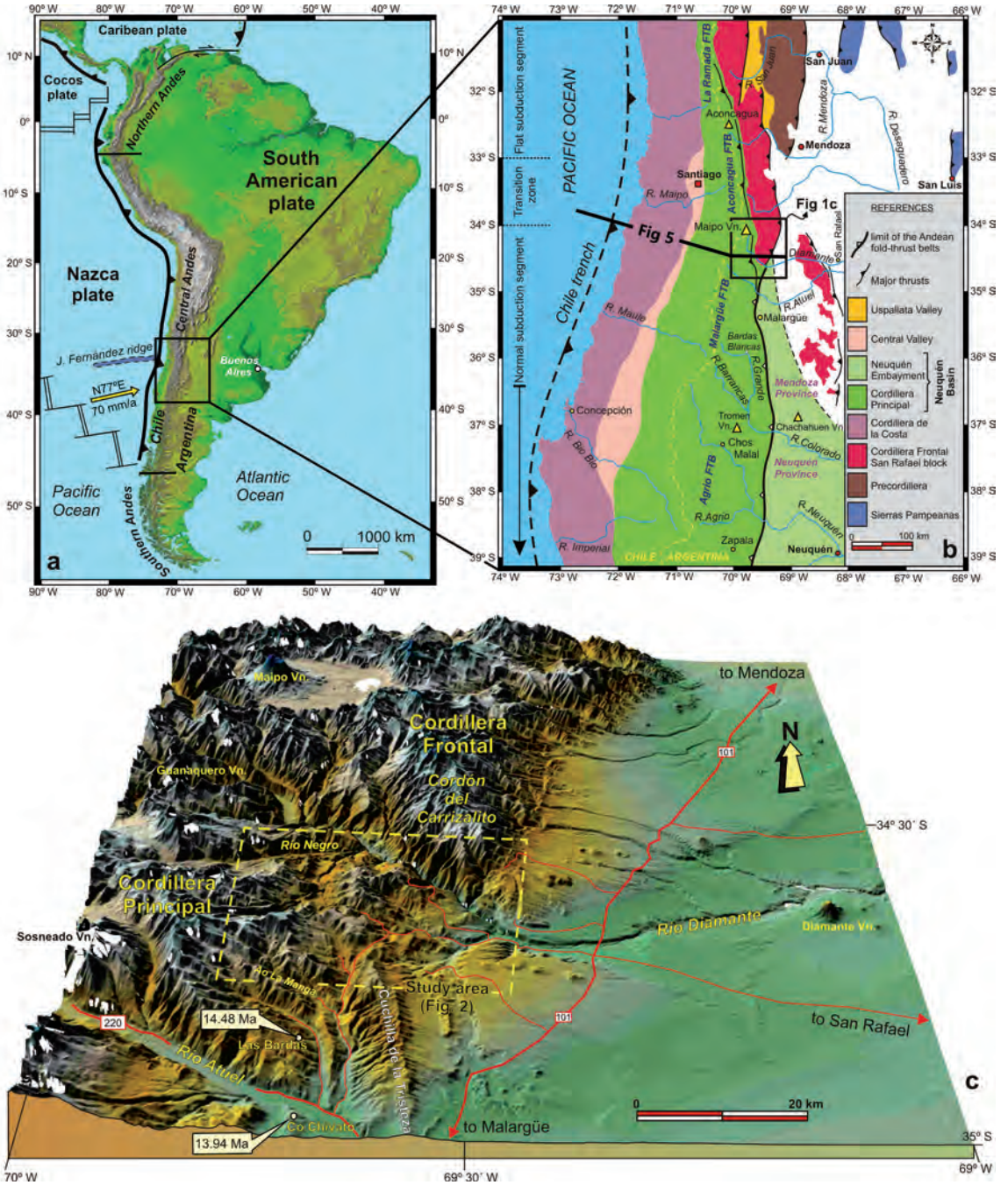

FIG. 1. **a.** Location of the studied region in the South Central Andes. The present day Nazca-South America convergence rate at ~35°S is 70 mm/a in the direction N77°E, calculated from the UNAVCO Plate Motion Calculator (http://sps.unavco.org/crustal_motion/dxdt/nnrcalc/); **b.** Main morphostructural provinces in the Andes of central-west Argentina based on Caminos (1979), Ramos (1988); Ramos *et al*. (2002), Ramos and Kay (2006); **c.** Digital elevation model (SRTM, 90m) of the Cordillera Principal and Cordillera Frontal in the studied area, between the Río Atuel and the Río Diamante. Shown ages of 14.48 Ma and 13.94 Ma, north and south of the Río Atuel, are from Giambiagi *et al*. (2008) and Baldauf (1997) respectively.

and some of these granitoids constitute very important porphyry Cu (-Mo) deposits (Maksaev *et al*., 2003; Deckart *et al*., 2010; Piquer *et al*., 2010). Geodetic models based on GPS estimations reveal that the current convergence rate between the Nazca and South American plates in this segment of the Andes is around 70 mm/a (Norabuena *et al*., 1999; Kendrik *et al*., 2003).

3. Stratigraphy

In the Río Diamante region, a suite of very different rocks compose the geological record, including: Paleozoic sedimentary and Permian-Triassic igneous rocks grouped as pre-Jurassic basement, Mesozoic sediments that filled the Neuquén basin and Cenozoic synorogenic sediments deposited together with volcanic and subvolcanic rocks during the Andean orogeny (Fig. 2). Early geological surveys in this relatively inaccessible portion of the Andes (Gerth, 1931; Groeber, 1947), has provided the basis for subsequent regional studies (Volkheimer, 1978; Sruoga *et al*., 2005), which constitute the essential geological background for current research. Figure 3 summarizes the nomenclature, lithology, thickness, age and tectonic setting of the geological units exposed in the studied area and they are briefly described below.

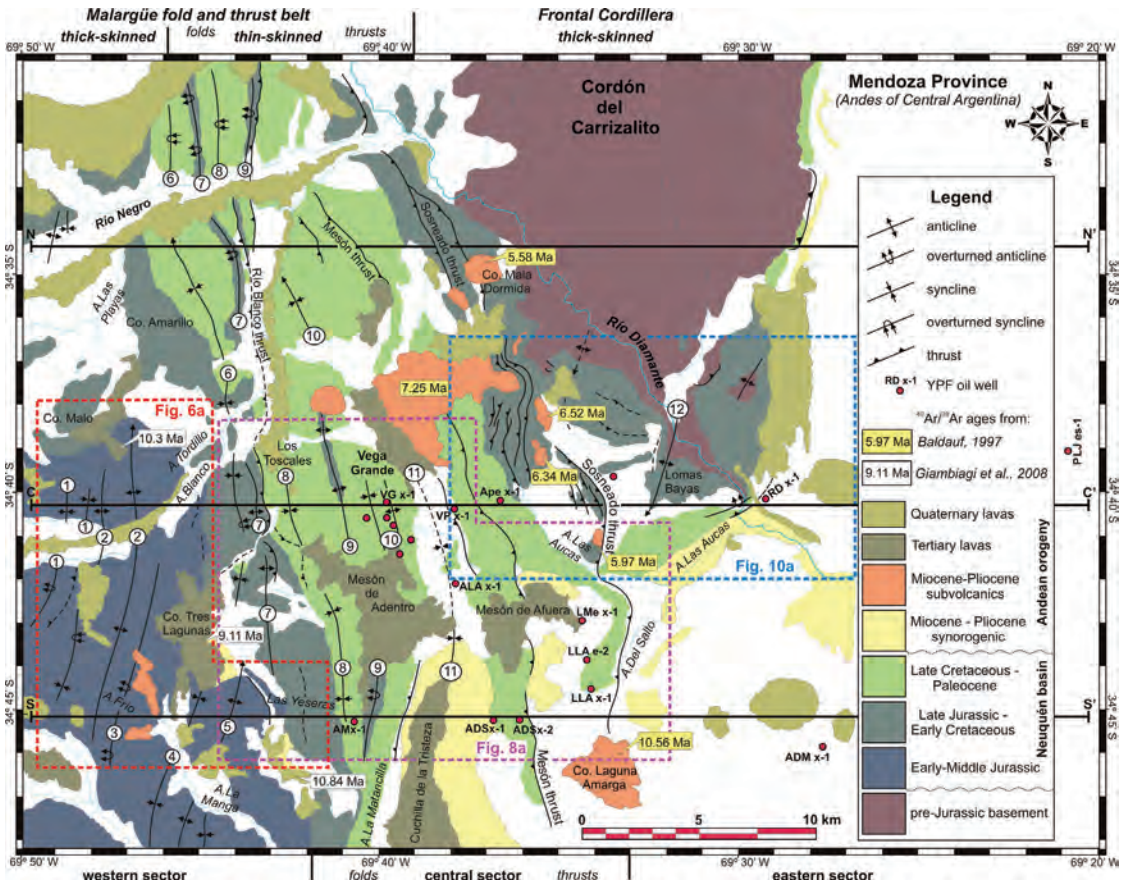

FIG. 2. Geological map of the Río Diamante region simplified from Turienzo (2008), with the structural domains established for this portion of the Malargüe FTB and the Cordillera Frontal. Numbers in circles correspond to the main folds in the area. **1.** Cerro Malo anticlines and synclines; **2.** Arroyo Tordillo anticlines; **3.** Arroyo Frío anticline; **4.** Tres Lagunas syncline; **5.** Las Yeseras anticline; **6.** Loma de las Mulas syncline; **7.** Río Blanco anticline; **8.** Los Toscales syncline; **9.** Vega de los Patos anticline; **10.** Vega Grande anticline and syncline; **11.** Cuchilla de la Tristeza syncline; **12.** Lomas Bayas anticline. Numbers in boxes are ages of Cenozoic volcanic and subvolcanic rocks from Baldauf (1997) and Giambiagi *et al.* (2008).

3.1. Pre-Jurassic basement rocks

Basement rocks are notably well exposed along the Río Diamante valley and toward the north in the Cordón del Carrizalito, an elevated range that forms the southern segment of the Cordillera Frontal (Fig. 2). The oldest unit is the Las Lagunitas Formation (Volkheimer, 1978), composed by a clastic succession of black shales and sandstones, partially metamorphosed, probably of Late Ordovician age (Tickyj *et al*., 2009). Magmatism related to subduction at the end of the Paleozoic in the continental margin of Gondwana produced granodiorites and tonalities grouped as Tonalita Carrizalito, with a K/Ar age of 334 Ma (Dessanti and Caminos, 1967), which intruded the preceding unit. Widespread Permian-Triassic magmatism of the Choiyoi cycle (Llambías *et al*., 1993) is represented by intermediate to acid volcanic, pyroclastic and plutonic rocks. In the studied area outcrops of granitoids prevail over volcanic and sedimentary rocks and thus the basement shows a noticeable rigid behavior during the Cenozoic Andean deformation, as revealed by micro and mesoscale studies (Turienzo *et al*., 2006), coherently with a thin overburden due to the reduced Mesozoic sedimentary cover developed in this marginal portion of the Neuquén basin.

3.2. Mesozoic sedimentary rocks of the Neuquén basin

The Jurassic-Cretaceous infill of the Neuquén basin took place by means of several sedimentary cycles (Groeber, 1947) or depositional sequences (Legarreta and Gulisano, 1989) that originated a heterogeneous stratigraphic succession characterized by an alternation of continental clastic sediments, shallow to deep-water marine deposits and evaporites. The numerous sedimentary units recognized on the field were integrated within three chronological intervals in order to simplify the regional map of the Río Diamante area (Fig. 2). In the studied region, the Jurassic-Cretaceous units show significant changes in their sedimentary facies and thickness toward the east, where the formations are thinner or absent (Fig. 3). Moreover, the total thickness of the Mesozoic stratigraphic sequence is notably reduced towards the foreland, from approximately 3,000 m in the west to lesser than 100 m in the east, as it can be appreciated in the YPF.PLJ.es-1 oil well (Fig. 4) and other neighboring exploration wells.

3.2.1. Early-Middle Jurassic

The initial infill of the Neuquén basin in the studied area is represented by the Cuyo Group, cropping out in the southwest region (Fig. 2), although these sediments are well-exposed and better known in the region of the Río Atuel, farther south (Volkheimer, 1978; Gulisano and Gutiérrez Pleimling, 1994; Lanés, 2005; Spalletti *et al*., 2005; Lanés *et al*., 2008). The oldest unit corresponds to the El Freno Formation (Hettangian-Sinemurian), mostly composed of coarse conglomerates and sandstones of fluvial origin, accumulated during the rifting stage of the Late Triassic-Early Jurassic extension. Faults controlling the subsidence in these rift systems are considered to be responsible of large thickness variations of the El Freno Formation (Giambiagi *et al*., 2005a, 2005b; Lanés, 2005; Lanés *et al*., 2008), although Spalletti *et al*. (2005) mentioned a uniform thickness of approximately 250-300 m throughout this region which cast doubt about the importance of such rift faulting. This unit is covered by the Puesto Araya and Tres Esquinas Formations, a fining upward sequence that begins with sandstones and concludes with black shales bearing ammonites and other marine fossils that represent the maximum marine expansion reached during the Bajocian. The Tábanos Formation (Middle Callovian), composed of evaporites and stromatolitic limestones formed in hypersaline shallow water conditions (Legarreta and Gulisano, 1989), represents a sudden sea level fall.

The Lotena Formation (Late Callovian) contains eolian and fluvial sandstones, which follows upwards with marine sandstones indicating a period of relative sea level rise (Gulisano and Gutiérrez Pleimling, 1994). Shallow marine conditions continued with the accumulation of the La Manga Formation (Early Oxfordian), composed of shelf carbonates facies, and the Auquilco Formation (Late Oxfordian), represented by thick evaporitic deposits. The Lotena, La Manga and Auquilco Formations comprise the Lotena Group (Fig. 3).

3.2.2. Late Jurassic-Early Cretaceous

A total desiccation of the basin occurred after the deposition of the Oxfordian evaporites as evidenced by the Tordillo Formation (Kimmeridgian), which shows a thick sequence of mainly fluvial red beds indicating a progradation of continental facies over marine rocks. Extensional tectonics with normal faults controlling thickness variations within this

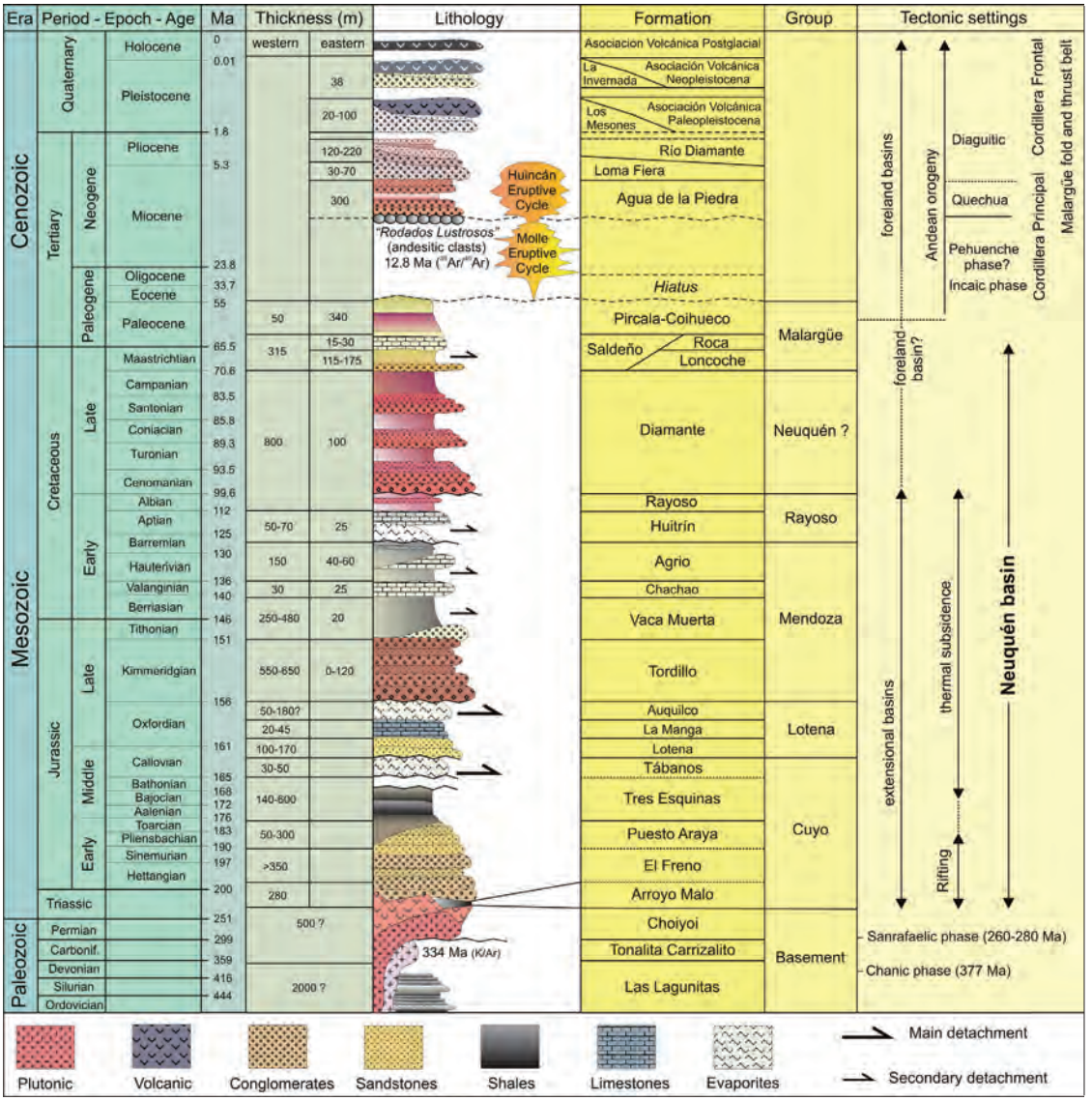

FIG. 3. Stratigraphic column showing the nomenclature, lithology, thickness, age and tectonic setting of the geological units exposed in the studied area. Arrows indicate detachment levels within the cover rocks.

unit, maybe as reactivations of the pre-existing Late Triassic-Early Jurassic rifting faults, has been proposed in the Aconcagua FTB (Giambiagi *et al*., 2003) and the Malargüe FTB (Mescua *et al*., 2008). The Vaca Muerta Formation (Tithonian), mostly composed of black shales, represents a sudden flooding of the Neuquén basin that took place when the rising sea level reached the threshold that separated the basin from the open sea (Gulisano and Guttiérrez Pleimling, 1994). The thickness and facies of this unit vary notably (Fig. 3), from 250-480 m of black shales in the west to only 20 m of conglomerates in the region of Lomas Bayas (Volkheimer, 1978; Tunik *et al*., 2005). The Chachao Formation (Valanginian) is formed by fossiliferous carbonates indicating a regional relative fall of the sea level, which has an almost constant thickness of 25-30 m throughout the studied area. On top of this horizon, the Agrio Formation (Late Valanginian-Early Barremian), containing 150 m of black shales and marls in the

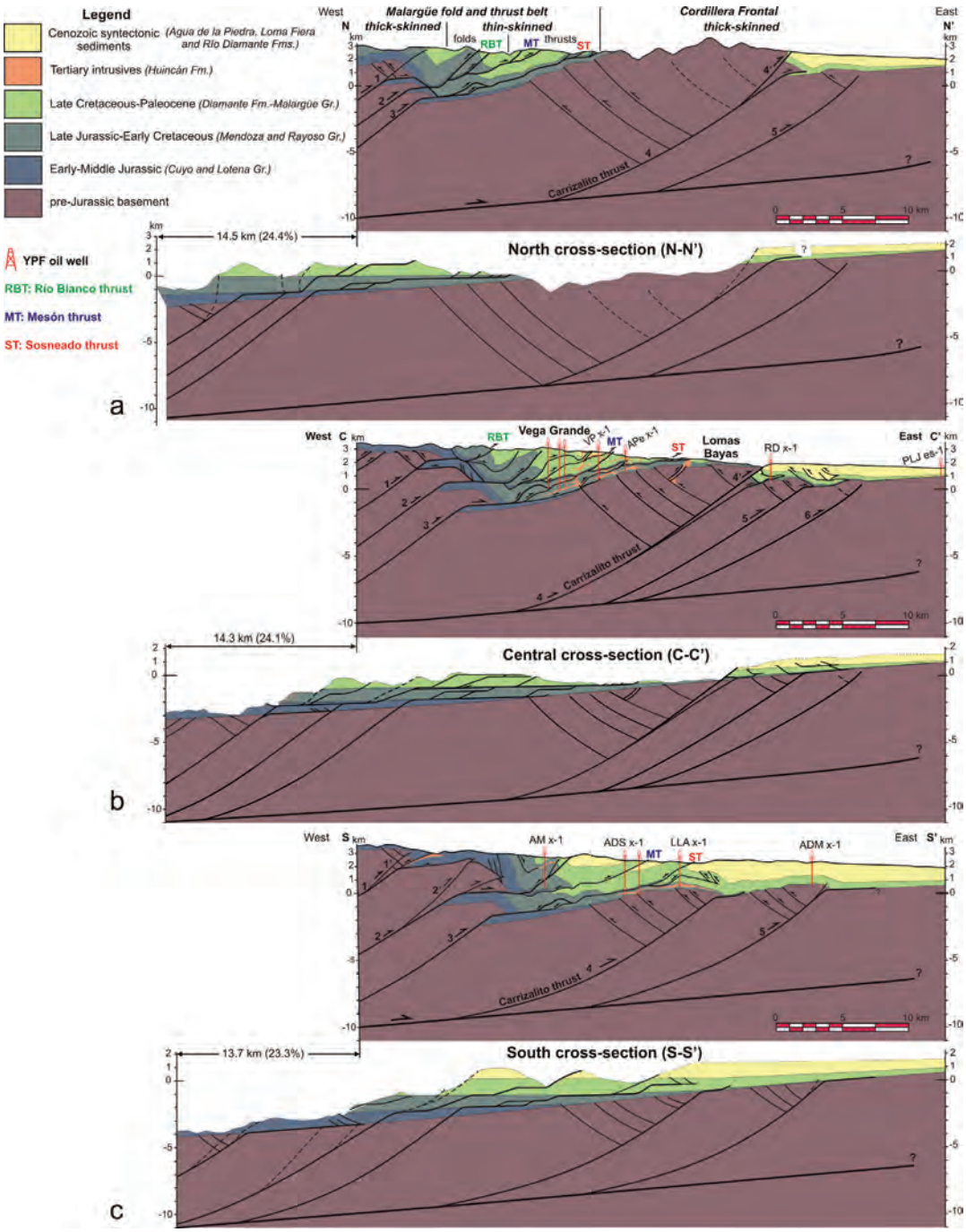

FIG. 4 **a, b, c.** North, Central and South balanced structural cross-sections across the thick and thin-skinned sectors of Malargüe FTB and the basement-involved structure forming the Cordillera Frontal, in the Río Diamante area (after Turienzo 2008, 2010). Stacked basement wedges related to low-angle thrusts faults formed during the Andean compression were responsible of the high structural relief (~3-6 km) and the exposure of Lower Jurassic rocks in the western sector. These wedges transmitted their displacement to the cover producing the folds and thrusts in the thin-skinned central sector. Lack of favourable detachment levels within the cover rocks in the eastern sector precluded the development of large basement wedges and instead important backthrusting occurred. The Carrizalito thrust breaks through to the surface thrusting pre-Jurassic and Mesozoic over Cenozoic rocks in the North and Central cross-sections, while in the South cross-section it remained as a blind thrust.

western sector and ~50 m of calcareous facies in the eastern region (Tunik *et al*., 2005), represents the last marine inundation from the Pacific Ocean in the Neuquén basin. All these formations constitute the Mendoza Group (Fig. 3).

The Huitrín Formation (Late Barremian-Aptian) includes evaporites in the inner sectors of the basin and carbonates in the marginal portions, evidencing a strong retreat of the sea. These deposits are covered by the Rayoso Formation (Albian), a fine-grain reddish clastic sequence that indicates a period of continental deposition, which together with the Huitrín Formation form the Rayoso Group.

3.2.3. Late Cretaceous-Paleocene

The accumulation of sediments in a continental environment continued during the Late Cretaceous with the Diamante Formation (Cenomanian-Campanian), a thick succession of red conglomerates, sandstones and claystones, which has variable thickness from ~800 m in the west to ~100 m in the east (Cruz, 1993). This unit is separated from the underlying strata by a regional unconformity (Legarreta and Uliana, 1991; Gulisano and Gutiérrez Pleimling, 1994) and it has a prograding character toward the foreland with internal sedimentary evidences of contemporaneous deformation (Kim *et al*., 2005; Orts and Ramos, 2006), which suggest accumulation in a compressive foreland basin formed by flexural deformation related to thrust belt loading (Ramos, 1988; Tunik et al., 2010).

The Loncoche Formation (Maastrichtian), composed of reddish and greenish conglomerates, sandstones and claystones corresponding to fluvial-lacustrine environments, overlie the Diamante Formation. Persistence of flexural subsidence in the Andean retroarc favors a shallow-marine transgression from the Atlantic Ocean represented by the Roca Formation (Campanian-Maastrichtian), which contains fossiliferous carbonates. The Pircala and Coihueco Formations (Paleocene) include fine-grained sediments with subordinated pyroclastic material, which indicate a progradation of continental over marine environments contemporaneously with an active volcanic arc located southward of the study area.

3.3. Andean Cenozoic rocks

The absence of Eocene sedimentary and volcanic rocks in this portion of the Andes marks an important hiatus (~20 Myr) after the deposition of the Paleocene Pircala-Coihueco Formations suggesting a regional uplift process (Legarreta and Uliana, 1991) followed by a period of compression that generated a widespread regional unconformity (Charrier and Vicente, 1972; Ramos, 1988; Charrier *et al*., 1996). The Cenozoic geological record in the studied area is intimately related to the tectonic evolution of the fold-and-thrust belt and to the evolution of the coeval magmatic arc.

3.3.1. Cenozoic magmatism

The magmatic activity in southern Mendoza during the Cenozoic can be separated in two eruptive cycles (Nullo *et al*., 2002), starting with the evolution of the Late Oligocene-Middle Miocene retro-arc magmatism of the Molle Eruptive Cycle (MEC) followed by the Middle-Late Miocene magmatic arc of the Huincán Eruptive Cycle (HEC). Large amounts of basalts exposed in the south of the Mendoza province, out of the study area, represent the MEC, with $^{40}Ar/^{39}Ar$ ages ranging from 24 to 13 Ma (Nullo *et al*., 2002; Combina and Nullo, 2011). Subvolcanic rocks exposed in the Las Bardas creek, to the north of the Río Atuel (Fig. 1c), were dated at 14.48±0.61 Ma by Giambiagi *et al*. (2008) and can be included within this cycle. The activity of the HEC occurred in two separate but related magmatic episodes distinguished as Huincán and La Brea Andesites (Nullo *et al*., 2002). The Cerro Chivato, to the south of the Río Atuel (Fig. 1c), is an andesitic body with related dykes of 13.94±0.08 Ma that represents the first magmatic pulse (Baldauf, 1997). According to $^{40}Ar/^{39}Ar$ data from this author, the second magmatic episode took place from 10.5 Ma to 5.5 Ma producing the emplacement of subvolcanic rocks several kilometers to the east as those located between the Cerro Laguna Amarga and the Cerro Mala Dormida (Fig. 2). Widespread coeval volcanic rocks (Basalts and Andesites) forming flat hills as the Cerro Tres Lagunas (Fig. 2), have $^{40}Ar/^{39}Ar$ ages between 10.84±0.52 Ma and 9.07±0.24 Ma (Giambiagi *et al*., 2008).

3.3.2. Neogene synorogenic sediments

Sedimentation related to the Andean mountain building started with the accumulation of the informally called 'Rodados Lustrosos' (Groeber, 1947; Yrigoyen, 1993), a conglomeratic level with clasts of volcanic rocks, at the base of the Agua de

la Piedra Formation. This unit is a heterogeneous set of interbedded conglomerates and sandstones in reddish colors, with variable thicknesses, which represent coalescent alluvial fans, fluvial systems and aeolian deposits (Combina and Nullo, 2005). The radiometric age of theses volcanic clasts range between 13.44±0.08 Ma and 12.83±0.1 Ma (Baldauf *et al*., 1992), thus accumulation of the synorogenic strata of the Agua de la Piedra Formation began after the Middle Miocene linked to the main deformation in this sector of the Andean fold-and-thrust belt (Baldauf, 1997; Combina and Nullo, 2005). Since this formation contains Oligocene mammalian fossils in the south of Mendoza province (Yrigoyen, 1993), a diachronic character along the Malargüe FTB has been proposed (Combina and Nullo, 2008, 2011). Further compression folded the strata of Agua de la Piedra Formation and consequently the upper contact with the Loma Fiera Formation is discordant. The Loma Fiera Formation is made up of lapilli tuffs, agglomerates, tuffaceous sandstones and conglomerates, which were generated by a sequence of primarily dry pyroclastic flows and their correlated lahars (Combina and Nullo, 2000). Pumice clasts were dated constraining the age of this unit to younger than 9.51±0.07 Ma (Baldauf, 1997). The Río Diamante Formation (Late Miocene-Pliocene?), which lies transitionally over the Loma Fiera Formation, is a sequence of volcaniclastic sandstones and conglomerates with a thickness of more than 120 m (Combina *et al*., 1993) interpreted as medium to distal sequences of alluvial fans, with subordinated ignimbritic, laharic and aeolian levels (Combina and Nullo, 1997, 2005).

4. Structure

4.1. Field observations and balanced cross-sections

Detailed field mapping in the region of the Río Diamante, between the Río Negro and the Arroyo La Manga (Fig. 1c), allowed us to recognize a variety of tectonic structures formed during the Andean orogeny (Fig. 2). With the aid of numerous 2D seismic lines and oil wells, Turienzo (2008, 2010) has made three E-W oriented balanced cross-sections (Fig. 4), normal to the main N-S trend of the Andean structures. The geometry of the basement-involved structure related to the Carrizalito thrust along the Central cross-section (Fig. 4b) is the best constrained due to both subsurface and field data. Considering the shortening (~3 km) and the excess area (~23 km^2) produced by this structure, Turienzo (2008, 2010) calculated a depth to detachment of 7.66 km from the top of the basement that is approximately 10 km below the sea level (Fig. 4). Applying this depth to the main detachment, the excess area was used to calculate the basement shortening related to the Carrizalito thrust in the North and South cross-sections (Figs. 4a and 4c). This main detachment is interpreted as dipping approximately 4-5° to the west (Turienzo, 2010), so the depth to such level varies from 6 km in the eastern portion of the sections to 11 km in the western one (Fig. 4). Crustal seismicity beneath the Chilean side of the Cordillera Principal at this latitude evidences a major detachment level that is located at ~10-5 km depth and dips ~5°W (Farías *et al*., 2010). We integrated structural data from both sides of the Andes to create a crustal structural cross-section across the entire mountain belt (Fig. 5). Farías *et al*. (2010) proposed a major east verging ramp-detachment structure connecting the subduction zone with the cordillera (Fig. 5), transmitting part of the stress from the plate interface and controlling mountain-building tectonics, thus playing a key role in the Andean orogeny.

From a regional point of view, the structure of this sector of the Argentinean Andes involves two basement uplifts occurring at the western and eastern sectors surrounding a central sector of thin-skinned deformation (Fig. 4). The western thick-skinned and central thin-skinned sectors constitute the Malargüe FTB while the basement-involved eastern sector corresponds to the southern part of the Cordillera Frontal.

4.1.1. Thick-skinned sector of the Malargüe FTB

Although pre-Jurassic rocks are not exposed in the western portion of the studied area, an important elevation of the basement lifted Early-Middle Jurassic sedimentary rocks at high topographic levels (Figs. 2 and 4). Diverse models have been proposed in order to elucidate the thick-skinned structures of the Malargüe FTB and its interaction with the sedimentary cover, including: inversion of previous normal faults, generation of new low-angle thrust faults during Andean compression, or a combination of both mechanisms (see discussion and references in Turienzo, 2010). According to the

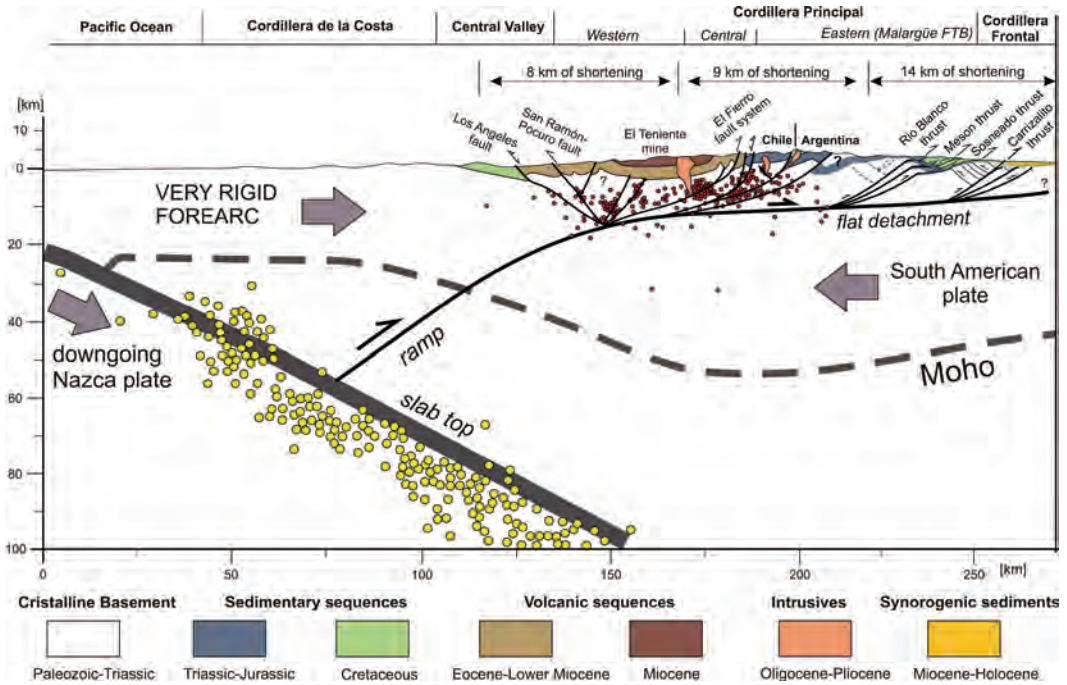

FIG. 5. Crustal cross-section across the Andes at ~34º-34º30' (see figure 1 for location) integrating the structures of the Chilean side from Farías *et al*. (2010) and the Argentinean side from Turienzo (2010). Based on crustal seismicity data beneath the Cordillera at this latitude Farías *et al*. (2010) proposed a major east verging ramp-detachment structure connecting the subduction zone with the cordillera. Shortenings estimated from structural cross-sections in the west and east flanks of the Andes at ~34°40'S are in the order of 17 km and 14 km respectively, which support a relatively symmetrical structural configuration of the orogen with a minimum total shortening of ~31 km.

inversion tectonics model, the Cenozoic contractional reactivation of pre-existing Mesozoic normal faults controlled the structural development of the Malargüe FTB (Manceda and Figueroa, 1995; Broens and Pereyra, 2005; Giambiagi *et al*., 2005a, 2008; Kim *et al*., 2005; Fuentes and Ramos, 2008; Mescua *et al.*, 2010). Analogue models show that contractional reactivation of extensional faults puts progressively older synrift strata into net contraction and suggest that total inversion has occurred if the null point is at the base of the synrift sequence and consequently the prerift layers have regained their pre-deformational regional elevation (Williams *et al*., 1989). Sandbox experiments were constructed to evaluate the role of pre-existing normal faults during the Andean mountain building, simulating the inversion of the Neuquén basin in the south of Mendoza province (Yagupsky *et al*., 2008) and the Abanico basin in the Chilean side of the Andes (Pinto *et al.*, 2010). Although many parameters controls the structural architecture in these models, like the orientation of the half-grabens respect to the compressive stress and the thickness of synrift sediments, they show that contractional strain is initially accommodated by reactivation of normal faults but commonly, after significant amounts of shortening, low-angle shortcut faults occur in the footwall accommodating major horizontal displacements. In recent structural reconstructions of the Malargüe FTB Giambiagi *et al.* (2009) show both pre-existing high-angle and new low-angle faults and analyze the mechanical properties of the rocks to evaluate the basement-cover interaction. In models that consider low-angle thrusting as the main mechanism contributing to mountain building during the Andean compression, the thick-skinned structures are commonly interpreted as large basement wedges or as first order fault-bend folds, which transfer their displacements along detachment horizons within the cover producing second order structures (Gerth, 1931; Dimieri, 1992a; Kozlowski *et al.*, 1996; Rojas and Radic, 2002; Turienzo and Dimieri, 2005a; Turienzo, 2008, 2010; Fortunatti,

2009; Torres Carbonell and Dimieri, 2011). In these models, the dominant N-S trend of the thrusts is in concordance with the Andean tectonic stress field and they are accountable for the significant horizontal shortenings that originate most of the structures observed in the cover rocks.

In the study region, despite that some authors interpret that reactivation of normal faults have occurred in the western sector affecting the Jurassic rocks (Giambiagi *et al.*, 2005a, 2008; Bechis *et al.*, 2010), we have not found supporting evidence indicating major tectonic inversion. Although the Mesozoic normal faults could have constituted weakness zones able to be reactivated during the subsequent compression, we think that the large structural relief at the thick-skinned sector of the Malargüe FTB, where the basement was uplifted almost 5 km from its undeformed position (Fig. 4), was more probably attained by stacking three thrust-related basement wedges that transmitted displacement to the cover as proposed by Turienzo (2010). These wedges have a lower detachment within the basement (~10 km) and an upper detachment in the cover, along the evaporites of the Tábanos and Auquilco Formations, constituting basement-involved duplexes (Fig. 4). A similar model of stacked basement structures was proposed for the region of Bardas Blancas, in the southern segment of the Malargüe FTB (Fig. 1b), where the YPF. BaB.x-1 oil well registered the presence of several slices of the Choiyoi Group (Manceda *et al.*, 1992). Comparable kinematic models, where superposition of basement-involved thrust sheets results in high elevations of basement rocks that produced deformation in the sedimentary cover, have been proposed in other fold and thrust belts in the Andes (*e.g.*, Kley, 1996; McQuarrie *et al.*, 2008) and elsewhere (*e.g.*, Schönborn, 1999; Heermance *et al.*, 2008).

Above the basement uplift of the western sector of the study area, Early-Middle Jurassic rocks are affected by N-S to NNE trending folds (1 to 5) with axis plunging gently toward the north, which explains why these rocks are covered by younger deposits in the Río Negro area (Fig. 2). The westernmost of these structures are two anticline-syncline pairs (Cerro Malo folds), located to the south of Cerro Malo, folding the Tres Esquinas and Tábanos Formations (Fig. 6a). The Cerro Malo folds were interpreted by Turienzo and Dimieri (2005a) as trishear fault-propagation folds considering both thin and thick-skinned deformation, resulting more suitable the reconstruction that involves basement rocks. The most noticeable structures in this sector are undoubtedly the Arroyo Tordillo anticlines (2 in Fig. 2), two westward-directed asymmetric anticlines with long, gently-dipping backlimbs (5º-15ºE) and short, steeply-dipping forelimbs (30º-40ºW), especially observed in layers of the El Freno Formation (Fig. 6b). These folds have straight flanks defining roughly a kink geometry and Turienzo (2010), based on similarities with other known basement-involved folds of west vergence, interpreted them as thick-skinned backthrusts-related anticlines (Fig. 4b). Toward the south, in the Arroyo Frío area, only one of these west-vergent anticlines was developed (Fig. 6a). In the backlimb of this anticline, east dipping strata abruptly become overturned forming the east-vergent Arroyo Frío anticline (Fig. 7a). This fold is related to a secondary thrust (1') that branches off from the thrust 1 associated with the uppermost basement wedge (Fig. 4c). Outcrops of the Early-Middle Jurassic rocks extend toward the east forming two open, northward-plunging folds (4 and 5 in Fig. 2): the Tres Lagunas syncline and Las Yeseras anticline (Fig. 6a). These structures were developed on the top of the second basement wedge and probably related to a branch (2') of the thrust 2 (Fig. 4c).

4.1.2. Thin-skinned sector of the Malargüe FTB

Ahead basement wedges of the thick-skinned sector, there is a ~15 km wide sector of thin-skinned deformation with a NNW orientation (Fig. 2). This sector can be subdivided in two regions with distinctly deformed cover rocks related to lithological variations according to its location within the basin. The important thickness of the stratigraphic pile with abundant shales and salt horizons at the west facilitated the formation of large fault-related folds whereas the thinner sedimentary cover located toward the east, bearing coarse-grain sediments and limestones, behaves more rigidly and thus it tends to form imbrications and duplex structures instead of significant folding (Fig. 4). Since the main detachments are the Middle Jurassic Tábanos Formation and the Early-Late Jurassic Auquilco Formation (Fig. 3), structures in the thin-skinned sector involve the sedimentary sequence younger than Middle-Late Jurassic.

4.1.2.1. Region of folds. The Loma de las Mulas syncline (6 in Fig. 2) is a broad structure that cons-

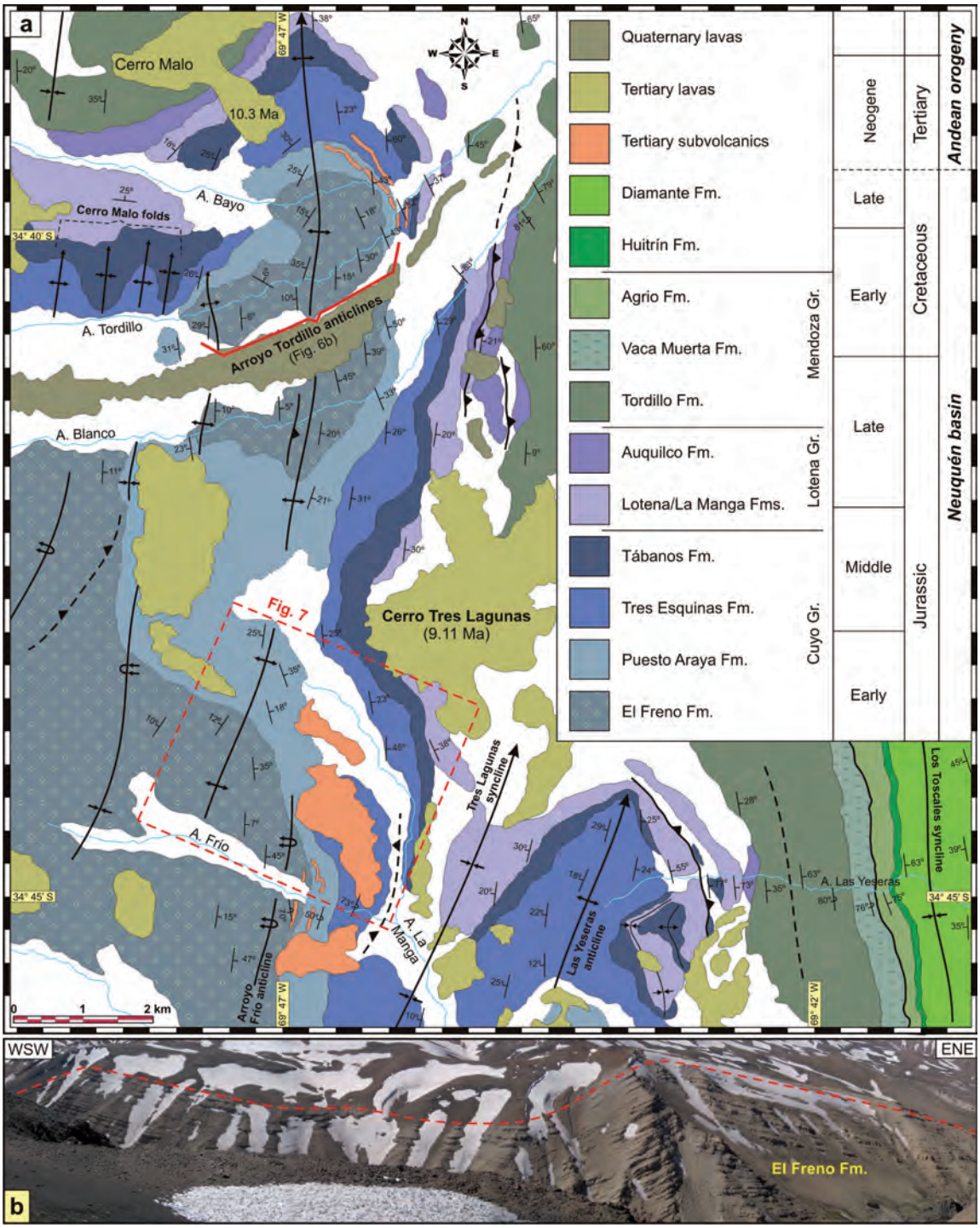

FIG. 6. **a.** Detailed map of the structures affecting Jurassic rocks in the southwest region of the studied area (see figure 2 for location); **b.** Panoramic photograph of the west-vergent Arroyo Tordillo anticlines characterized by long, gently-dipping backlimbs and short, steeply-dipping forelimbs.

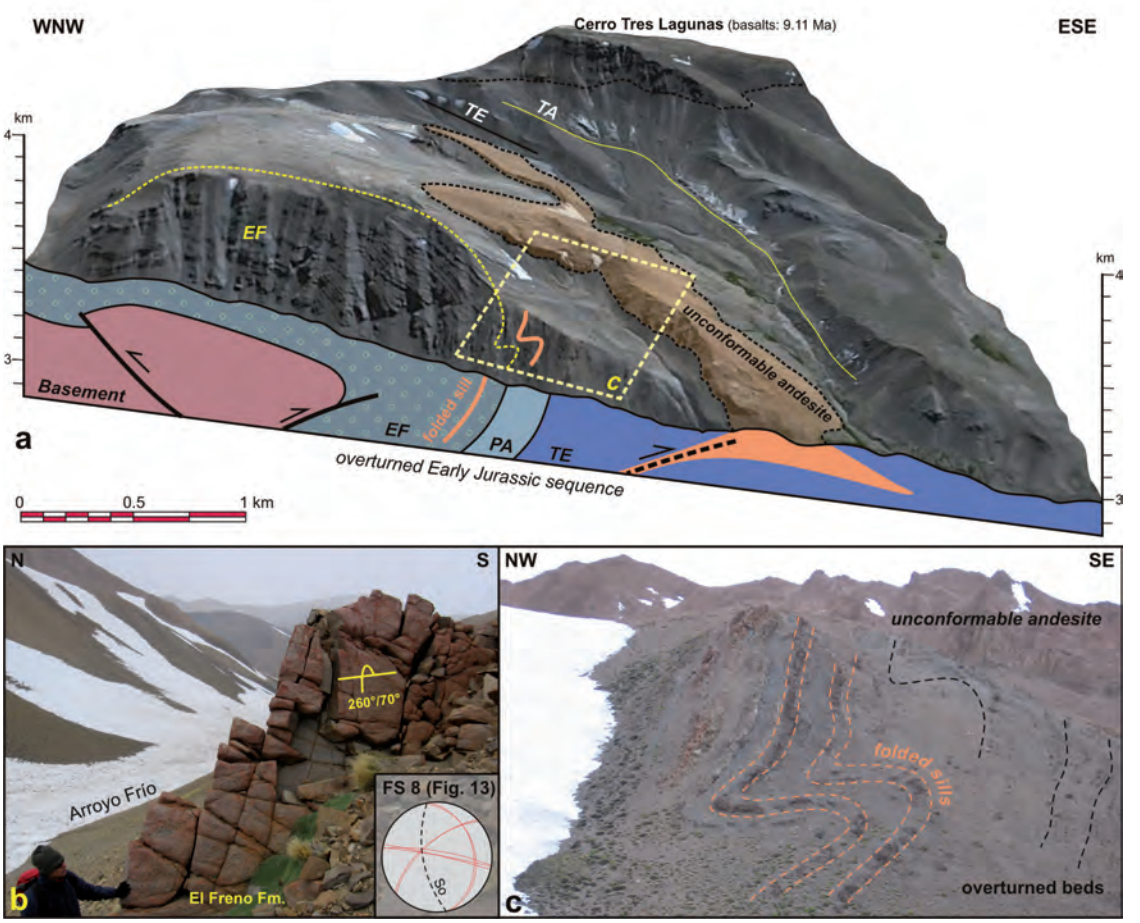

FIG. 7. **a.** Composite sketch across the east-vergent Arroyo Frío anticline (see figure 6 for location); **b.** Overturned and fractured conglomerate bed of the El Freno Formation, where fracture station 8 was recorded; **c.** Andesitic sills folded with the Jurassic sediments in the forelimb of the Arroyo Frío anticline, unconformably covered by younger subvolcanic rocks.

titutes the link between the thick and thin-skinned sectors of the Malargüe FTB (Fig. 4a). This fold is well developed along the north cross-section, where it reaches a maximum width of 5 km, and has the western limb dipping 50º-80ºE and the eastern limb dipping 40º-50ºW. The axis of the syncline plunges to the north and in the southern area, this fold becomes tighter and overturned. In front of the Loma de las Mulas syncline there are three kilometric-scale folds, which are completely exposed in the north side of the Río Negro valley where it is possible to observe two east-vergent anticlines with an overturned syncline linking them (7, 8 and 9 in Fig. 2). The westernmost fold is the Río Blanco anticline (7), which in the north cross-section was thrusted over the Los Toscales syncline (8) and the Vega de los Patos anticline (9) by means of the Río Blanco thrust (Figs. 2 and 4a). Turienzo (2010) interpreted this thrust, which placed the Río Blanco anticline over the younger folds situated to the east, as an out-of-sequence thrust. In the central cross-section the Río Blanco anticline involves the Mendoza Group, which was thrusted over the Diamante Formation red beds that form the Los Toscales syncline (Fig. 8a). The Río Blanco anticline was interpreted as created in two separated stages (Turienzo and Dimieri 2005a; Turienzo, 2010): an earlier fault-related fold with a lower detachment in the Jurassic evaporites, followed by a later episode of faulting when the Río Blanco thrust branched off from the ramp zone breaking through the forelimb of the anticline. The Los Toscales syncline extends from the Río Negro

to the Arroyo Las Yeseras (Fig. 2), for approximately 30 km, involving the Late Cretaceous Diamante Formation. The Vega de los Patos anticline (Fig. 8b) shows a similar continuity along strike and has an eastward vergence, clearly observed to the south of Cerro Mesón de Adentro (Fig. 8a) and to the north of Río Negro where the anticline is overturned and displaced toward the foreland by a west-dipping thrust (Fig. 2). Despite that the Vega de los Patos anticline affects the Cretaceous Huitrín and Diamante Formations at the surface, the YPF.AM.x-1 well located in its backlimb (Fig. 4c) verified that rocks as old as the Late Jurassic Tordillo Formation are involved in depth. Like the Río Blanco anticline, the Vega de los Patos anticline can be reconstructed in two stages including an open fault-bend fold that duplicated the Late Jurassic-Early Cretaceous rocks, which afterwards was affected by a second fault, increasing the forelimb dips and producing a tight fault-propagation anticline. Nevertheless, we made a kinematic reconstruction with the Pliegues2D software (Cristallini, 2005) considering a different sequence of events: an early fault-propagation fold that was transported over an upper flat detachment (Fig. 9). In this sequential reconstruction we show that the displacement transferred from the basement wedges of the thick-skinned sector produced the repetitions of the Late Jurassic-Early Cretaceous rocks, the folding structures (*e.g.* the Vega de los Patos anticline) and the repetitions of Late Cretaceous strata registered in the Vega Grande oil wells. As a result, the final geometry of the modeled structures (Fig. 9) is comparable with the structures exposed at this segment of the central cross-section (Fig. 4b). The antiformal stacking of the Late Cretaceous slices is represented in the surface by the Vega Grande anticline (10 in Fig. 2).

4.1.2.2. Region of thrusts. Thrusts in the thin-skinned zone of the Malargüe FTB have a general N-S trend that varies to NW-SE in the north, where they are affected by the basement-involved structure of the Cordillera Frontal (Fig. 2). These structures are composed of numerous low-angle faults developed in two defined fault systems, identified from west to east as Mesón thrust and Sosneado thrust (MT and ST in Fig. 4 respectively). The Mesón thrust is very well exposed surrounding the Cerro Mesón de Afuera (Fig. 8a) where it placed Late Cretaceous over Miocene rocks (Figs. 8c and 8d). In the northern area, the Mesón thrust produced imbrications within the Late Cretaceous rocks (Figs. 2 and 4a). The Cuchilla de la Tristeza syncline (11 in Fig. 2) is a broad N-S trending fold developed between the Mesón thrust and the Vega de los Patos anticline. This syncline has a maximum width of 5 km along the South cross-section, where it contains a thick succession of synorogenic Cenozoic rocks, and decreases toward the north where it is recognized by scarce outcrops of Late Cretaceous rocks nearby the Vega Grande oil field (Fig. 8a). The Sosneado thrust is observed affecting different units along strike related to the easternmost basement uplift (Figs. 2, 4 and 8). In the southern area, this thrust uplifted Late Cretaceous strata that dip 20°-30° W over Miocene strata dipping 10°-20° E (Fig. 8a). Toward the north, the Sosneado thrust affected intensely the Huitrín Formation (Fig. 10a), forming duplex structures (Fig. 10b).

4.1.3. Thick-skinned structures of the Cordillera Frontal

The Cordón del Carrizalito represents the southern part of the Cordillera Frontal and constitutes one of the most important morphological features in the studied area (Fig. 1c). This range is a huge anticlinorium, cored by pre-Jurassic basement rocks, which plunge toward the south until it disappears in the region of the Río Diamante (Fig. 2). Mesozoic sediments lay unconformably over the basement in the trailing edge of the Cordillera Frontal while its leading edge is limited by the ~N-S trending Carrizalito thrust, which locally reached the surface and thus the pre-Jurassic rocks were thrusted toward the foreland over the younger sedimentary rocks (Figs. 4a and 4b). This is particularly notorious near the confluence of the Arroyo Las Aucas with the Río Diamante (Fig. 10a), where the Carrizalito thrust uplifted both basement and Late Jurassic-Early Cretaceous rocks over the Miocene Agua de la Piedra Formation (Fig. 10c). The Mesozoic strata dipping ~12ºSE that are overlying the basement in the hangingwall of the Carrizalito thrust, abruptly become steeply-dipping to overturned and notably thinned close to the thrust. In the footwall, layers of the Agua la Piedra Formation have a maximum dip of 64ºSE that decrease considerably to the east away from the thrust. The YPF.RD.x-1 well data, which goes through the basement-cover contact in the footwall of the Carrizalito thrust, supports the estimation of a vertical offset of ~900 m (Fig. 10d). Turienzo and Dimieri (2005b) reconstructed accurately the rounded geometry of the fold depicted

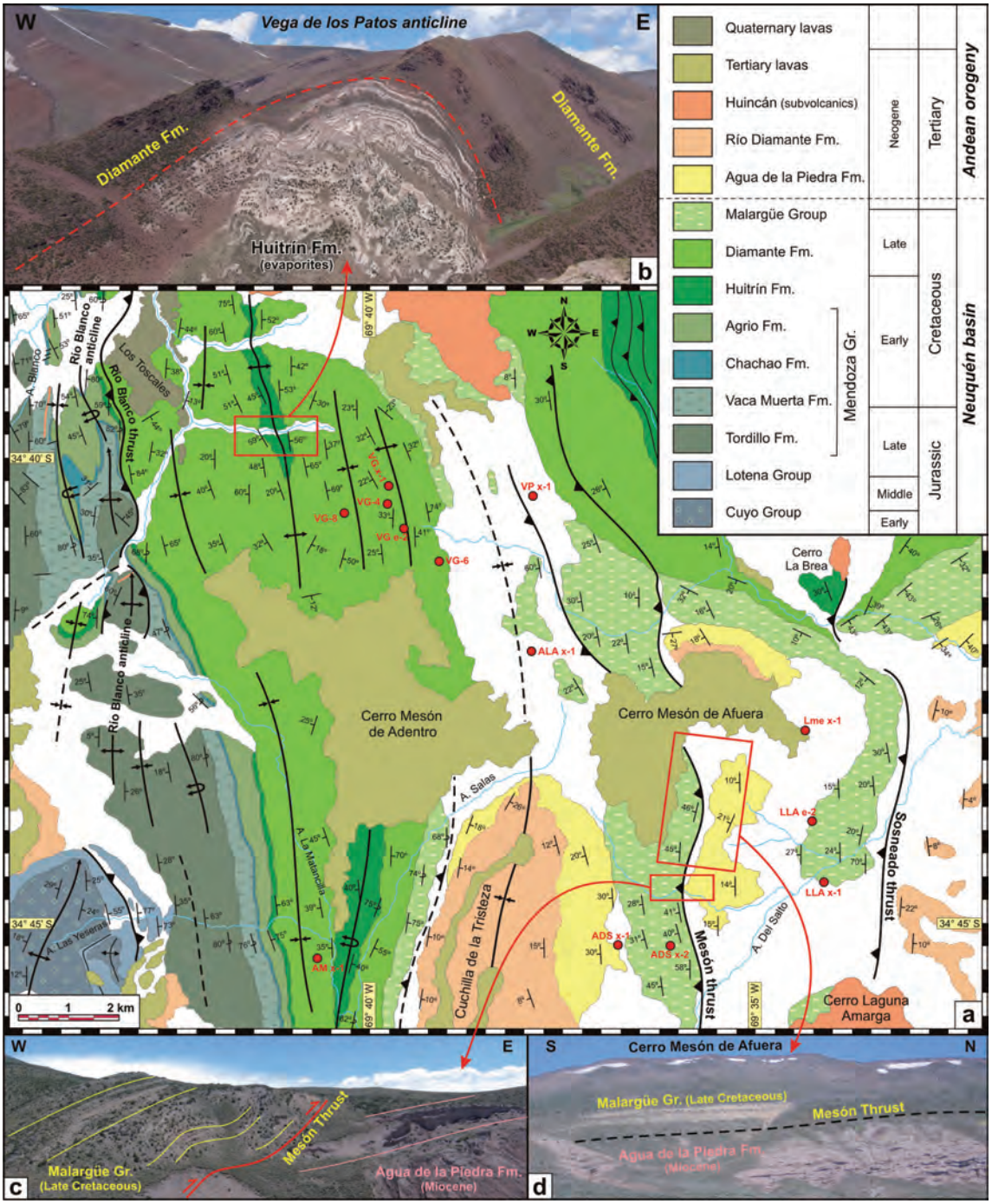

FIG. 8. **a.** Detailed map showing a portion of the thin-skinned central sector of the Malargüe FTB involving Upper Jurassic-Cretaceous sedimentary rocks (see FIG. 2 for location); **b.** Photograph of the east-vergent Vega de los Patos anticline, extraordinarily exposed due to the lithological contrast between the Huitrín Formation evaporites and the Diamante Formation red beds; **c-d**. Lateral and frontal views of the Mesón thrust placing Late Cretaceous over Miocene rocks.

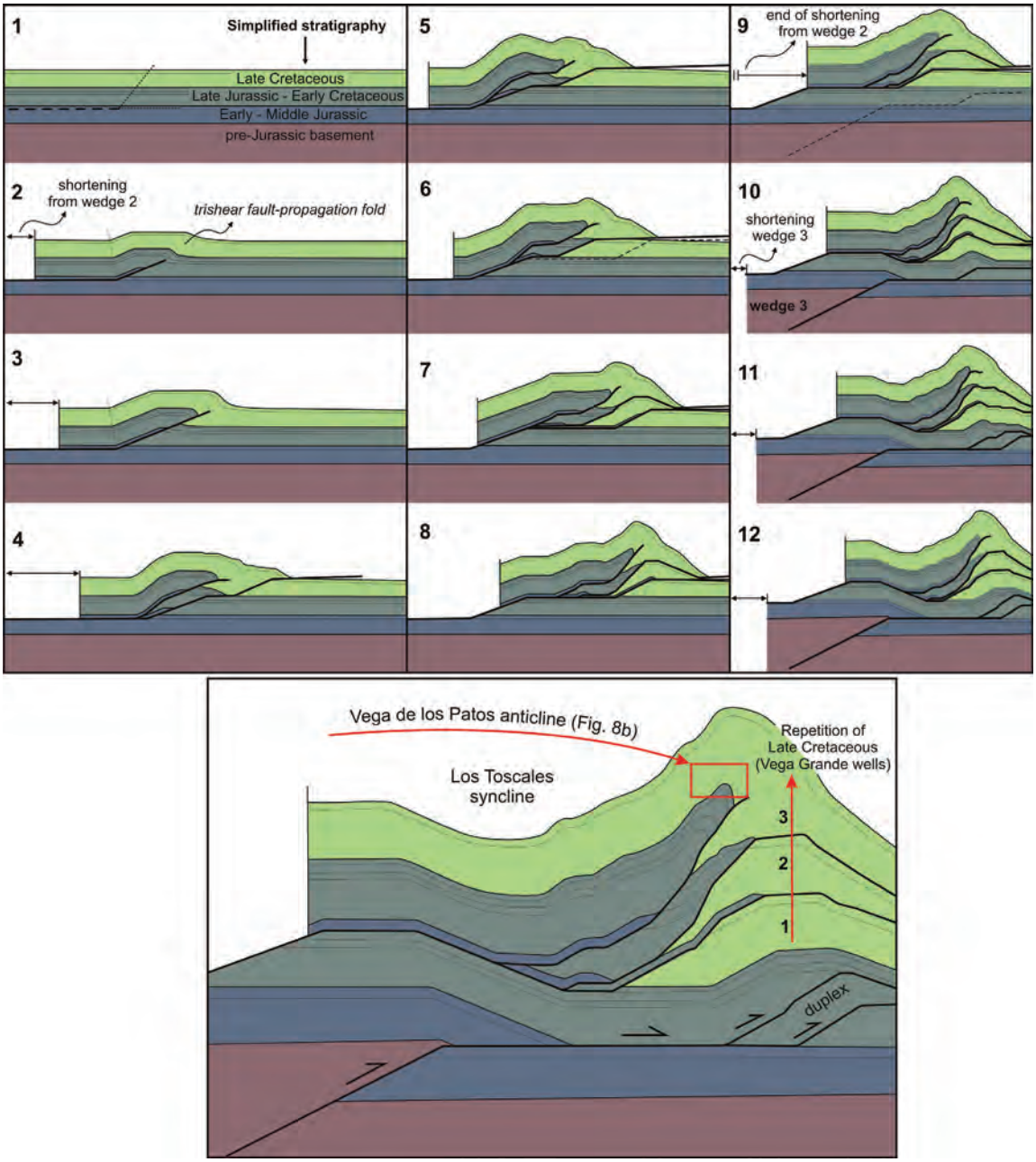

FIG. 9. Schematic kinematic reconstruction illustrating the basement-cover interaction to explain the development of the Vega de los Patos anticline as a trishear fault-propagation fold, afterwards transported over an upper decollement. Forward modelling was made with the Pliegues2D software (Cristallini, 2005).

by the sedimentary layers in front of the Carrizalito thrust interpreting this structure as a trishear fault-propagation fold, with a p/s ratio of 1.5 and a fault angle of ~40º (Fig. 10d).

The Lomas Bayas anticline (12 in Fig. 2), entirely exposed in the southwest side of the Río Diamante (Fig. 10a), is the most noticeable structure that forms part of the Cordón del Carrizalito anticlinorium. It

is a west-vergent asymmetric anticline, related to a backthrust that branches off from the Carrizalito thrust (Fig. 4b) and cored by pre-Jurassic basement rocks (Fig. 10e). The Lomas Bayas anticline has a short forelimb that dips 30º-35ºW and a longer backlimb that dips 8º-12ºSE, while the axis plunges ~11ºSSW. The basement-cover contact along the Río Diamante to the northwest of Lomas Bayas is inclined ~12º-14ºSE, while surrounding the Cerro Media Luna there are beds of the Vaca Muerta and Agrio Formations dipping 18º-24ºSW (Fig. 10a). These exposures roughly depict the hinge zone of a second backthrust-related anticline, which together with the Lomas Bayas anticline constitute a train of two asymmetric folds characterized by long, gently-dipping backlimbs and shorter, steeply-dipping forelimbs developed above a backthrust system as in the case of the Arroyo Tordillo anticlines (Fig. 6b). Turienzo and Dimieri (2005c, 2006) developed kinematic models in order to explain this particular geometry of basement-involved anticlines associated to backthrust systems. In such models, backthrusting occurs in order to accommodate deformation in the hangingwall of a main thrust when its forward movement is hindered.

Basement-involved structures at the eastern sector of the South cross-section, below the thin-skinned Mesón and Sosneado thrusts, were recognized by Turienzo (2008, 2010) from seismic and well data. They are represented by backthrusts in the hangingwall of the Carrizalito thrust, which in this cross-section remains as a blind thrust (Fig. 4c). The YPF.ADM.x-1 oil well located some kilometers toward the east detected the basement-cover contact forming the Del Medio anticline in a level higher than in the undeformed foreland, whose elevation is known from the YPF.EJ.es-1 well situated out of the studied area. Along the Central cross-section, if the basement-cover contact registered in the YPF.PLJ.es.1 is extended to the west with the regional slope, clearly results that the same contact registered in the YPF.RD.x-1 well is in a higher level, which lead us to interpret it as related to an incipient basement-involved structure formed to the east of the Carrizalito fault (Fig. 4b). In our interpretation, the deformation associated with this small basement wedge produced the westward-directed thrusts affecting Cenozoic rocks observed in the Río Diamante valley (Fig. 10f).

4.2. Variations along strike of the basement-involved structures

Based on the depth to the basement data from oil wells in the region and the geometry of the structures in cross-sections, Turienzo (2008, 2010) constructed a structural map showing the top of the pre-Jurassic basement (Fig. 11a). In order to visualize clearly the changes along strike of the thick-skinned structures in the studied area, we constructed a perspective view integrating the basement-involved structures of the three cross-sections (Fig. 11b). Stacking of three basement wedges generated the large structural relief at the western region, which reaches about 5.4 km (from -2,000 m to +3,400 m) in the South cross-section to about 3.2 km (from -1,200 m to +2000 m) in the North cross-section (Fig. 11). This variation in structural relief produces the plunge of the structures and the Early-Middle Jurassic rocks toward the north, where they are covered by younger sediments (Fig. 2). Backthrusts in the toe of the upper basement wedge are common structures in all cross-sections.

The height above sea level of the basement rocks in the eastern region varies considerably from north to south since they are exposed at ~3800 m in the Cordón del Carrizalito and were found at ~400 m in the YPF.LLA.x-1 well (Fig. 11). The structural relief associated to the Carrizalito fault, in comparison with the depth to the basement-cover contact in the footwall, is 2.7 km, 1.3 km and 0.6 km in the North, Central and South cross-sections respectively. The N-S trending seismic lines 5,085; 60, 5111-60 and 5,110-60, located between the Central and South cross-sections (Fig. 12a), show that the top of the basement is higher in the north side of the lines forming an important step of variable magnitude from west to east (Figs. 12b, 12c and 12d). Connecting these steps observed in the seismic lines together with the NE to ENE strike of the beds southward of Lomas Bayas (Fig. 10a), it is possible to identify a ~ENE trending zone of faulting interpreted as a lateral ramp of the Carrizalito thrust that explains the differential basement uplift between the north and south regions (Fig. 11). The displacement produced by this fault is small in line 5,085-60 (Fig. 12b) and increases considerably in line 5,111-60 where the southward-dipping reflectors are in agreement with the plunge of the Lomas Bayas anticline (Fig. 12c).

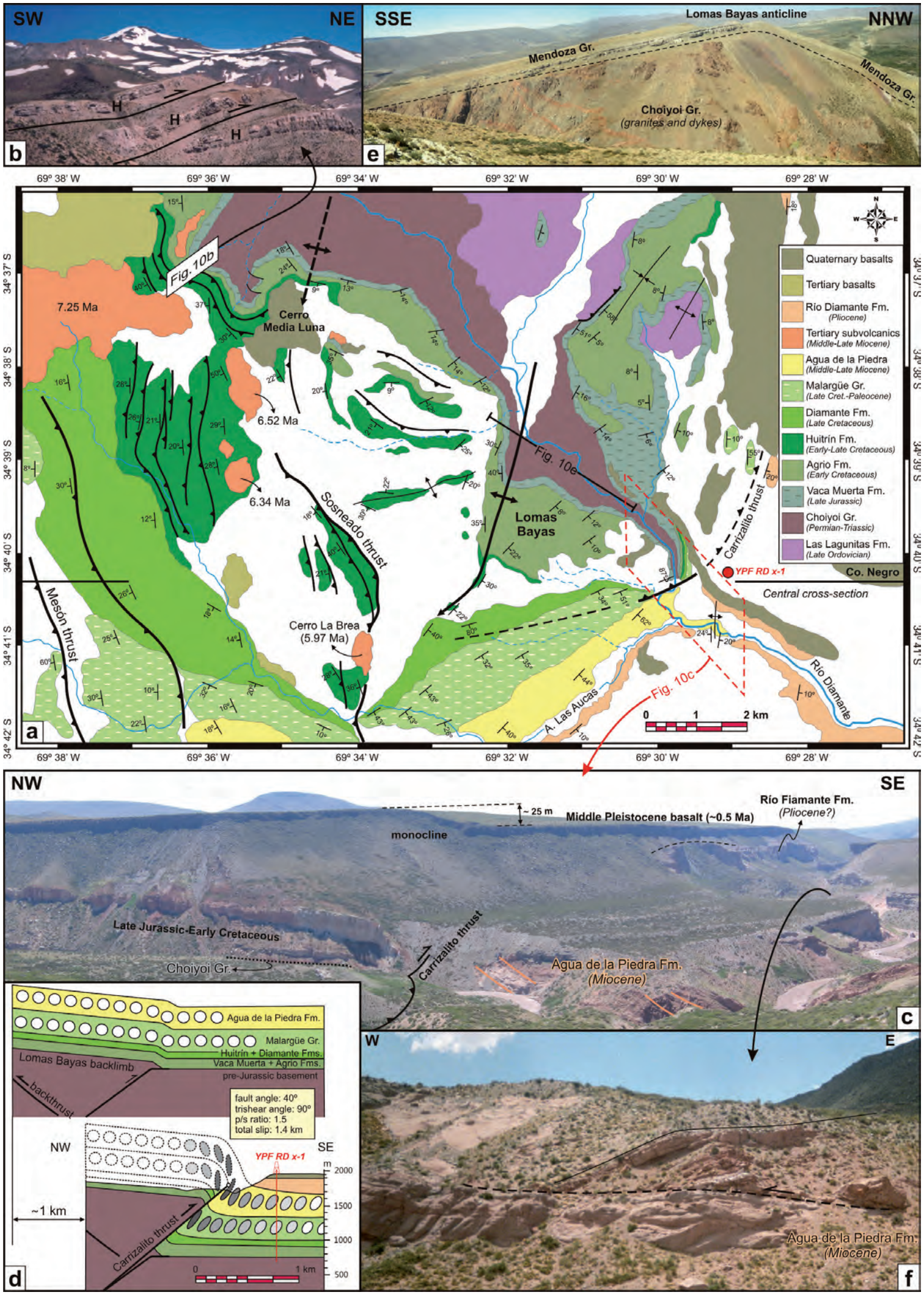

FIG. 10. **a.** Detailed map including the thrusting zone of the thin-skinned sector of the Malargüe FTB and the basement-involved structures of the Cordillera Frontal; **b.** Duplex structures related to the Sosneado thrust, involving limestones of the Huitrín Formation; **c.** Panoramic photograph of the Carrizalito thrust in the Río Diamante valley, which placed pre-Jurassic and Mesozoic over Cenozoic rocks; **d.** Kinematic reconstruction of the rounded fold associated to the Carrizalito thrust as a trishear fault-propagation fold; **e.** The west-vergent, basement-cored, Lomas Bayas anticline, viewed from the north side of the Río Diamante, which is associated to a backthrust that branches off from the Carrizalito thrust; **f.** West-vergent fault-bend fold in Miocene strata, located along the Río Diamante valley eastward of the Carrizalito fault.

There is a major displacement in line 5110-60 (Fig. 12d), which shows the faulted basement in the same manner as observed in the Río Diamante (Figs. 10a and 10c). These differential displacements along the fault define this lateral ramp as a rotational or scissor fault. Backthrusts affecting the basement rocks in the hanging wall of the Carrizalito thrust are present in all the cross-sections, even in the south where the fault remained as a blind thrust (Fig. 11).

4.3. Shortenings

Restitution of thin and thick-skinned structures of the cross-sections was made by Turienzo (2008, 2010) in order to calculate the respective tectonic shortenings and subsequently to compare them with other published studies of the Malargüe FTB. In each cross-section, basement and cover shortenings are comparable because the displacement from the basement-involved thrusts was consumed in the development of structures in the cover rocks, which implies a close temporal and spatial relationship between the thin and thick-skinned deformation.

The similarity in shortenings calculated from the North, Central and South cross-sections, 14.5 km (24.4%), 14.3 km (24.1%) and 13.7 km (23.3%) respectively (Fig. 4), demonstrate that a contraction in the order of ~14 km or 24% is reliable for this region of the Argentinean Andes (Turienzo, 2010). Despite the main thick-skinned structures vary considerably along strike, this consistency in the magnitude of shortening between all three cross-sections is due to a decreasing development of the thick-skinned structures from south to north in the western sector and an increment from south to north in the eastern sector (Fig. 11).

Recently published papers have proposed different crustal-scale models in order to elucidate the large-scale Andean structures and their dominant vergence, at this latitude of the Argentinean-Chilean Andes (Armijo *et al*., 2010; Farías *et al*., 2010). Based on geomorphological data evidencing that the east-dipping San Ramón fault is active and structural reconstructions of the Andean structures in Chile between 33° and 34°S, Armijo *et al.* (2010) proposed a west verging first-order tectonic model of the Andes involving an embryonic intracontinental subduction that would be a mechanical substitute of a collision zone, suggesting that the Andean orogeny paradigm is obsolete. Taking into account seismicity and surface geology, Farías *et al.* (2010) documented a major east verging ramp-detachment structure that connect the subduction zone with the cordillera, at which most of the Andean structures would be rooted, and it allows the distribution of crustal thickening in a 'simple shear deformation mode'. Beyond the huge differences between these crustal-scale models, and the discussible arguments supporting or rejecting each hypothesis (*e.g.*, Astini and Dávila, 2010), the structural cross-sections across the Chilean Principal Cordillera depict comparable shortenings of around 10-15 km (Armijo *et al*., 2010; Farías *et al*., 2010). Farías *et al*. (2010) established a significant structural asymmetry for the whole orogen at ~33.30°S comparing their own estimations of shortenings for the Chilean side, in the order of 16 km, with the ~60 km obtained by Giambiagi and Ramos (2002) in the Argentinean side across the Aconcagua FTB and the Cordillera Frontal. At ~34°40'S, Turienzo (2010) calculated ~14 km of shortening across the Malargüe FTB and the Cordillera Frontal and similar estimates were made by Dimieri (1992a), Giambiagi *et al*. (2008) and Fortunatti (2009) in different places along the southern portion of the Malargüe FTB. These values are comparable with the ~17 km of shortening in the Chilean side at this latitude (Farías *et al*., 2010), which support a relatively symmetrical structural configuration of the orogen in this segment of the Andes with a minimum total shortening of ~31 km (Fig. 5).

5. Analysis of fracture sets

Studies of fractures at mesoscopic scale are frequently used to analyze the stress-strain relationship in most orogenic areas since these structures are the most common response of rocks to brittle deformation. Exhaustive research have been made extensively in the Rocky Mountains (*e.g*., Erslev *et al*., 2004, Sanz *et al*., 2008; Amrouch *et al*., 2010) and in other regions worldwide (*e.g*., Knipe, 1990; Wibberley, 1997) about the linkage between the kinematics of basement-cored compressive structures and the behavior of such basement rocks during deformation, considering fracture patterns, minor faults and microstructures. Despite of its importance, kinematic analysis taking into consideration minor faulting and fractures in structures produced during the Cenozoic compression along the Argentinean Andes are notably scarce (Zapata *et al*., 2001; García

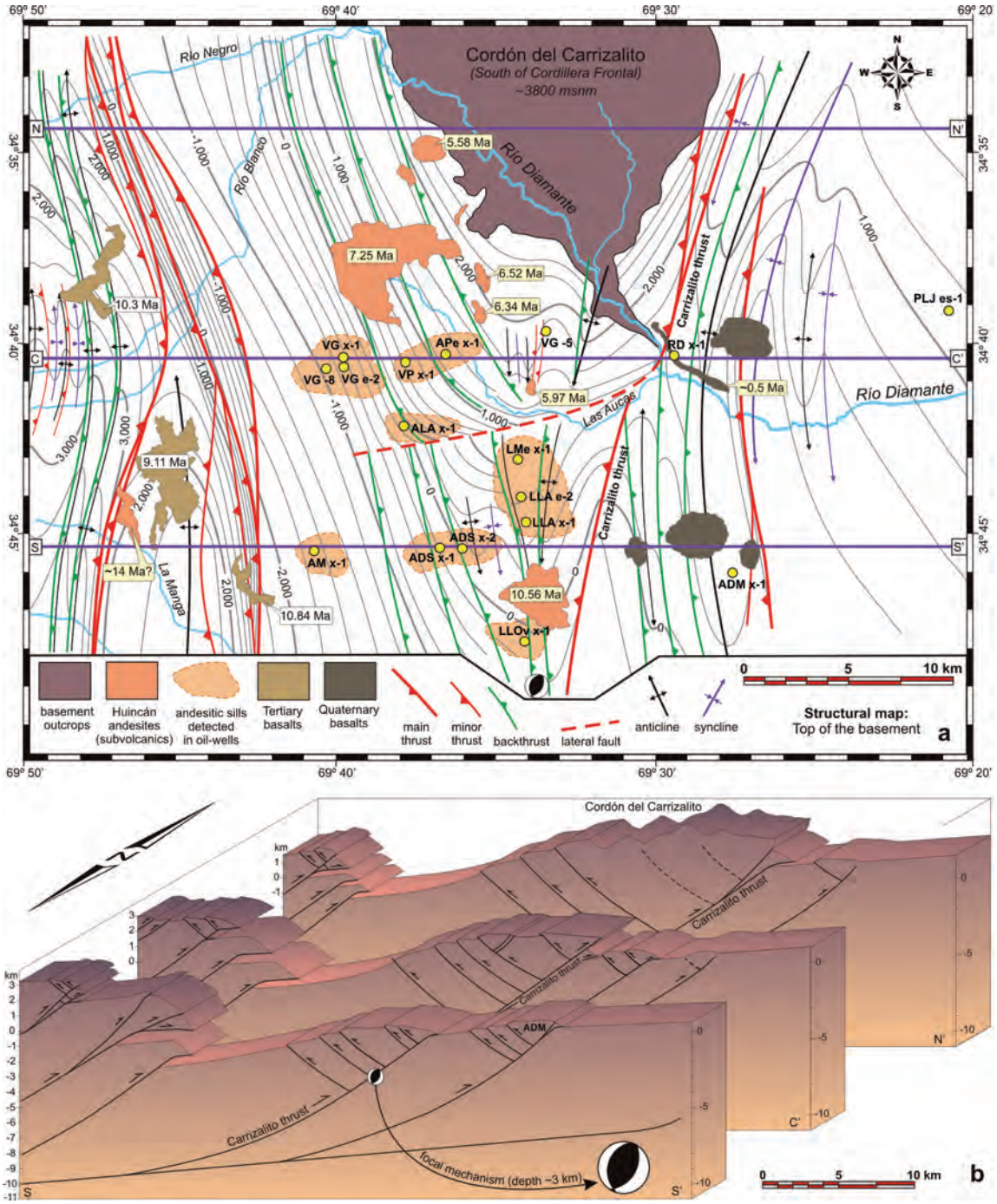

FIG. 11. **a.** Structural map constructed at the top of the pre-Jurassic basement, based on well data, seismic interpretation, and interpreted structural cross-sections (after Turienzo 2008, 2010). Contour interval is 200 m. The large structural relief caused by the stacking of basement wedges in the thick-skinned western sector varies from ~5.4 km in the South cross-section to ~3.1 km in the North cross-section. In the eastern sector, the structural reliefs associated to the Carrizalito thrust are 2.7 km, 1.3 km and 0.6 km in the North, Central and South cross-sections respectively. A lateral ramp was responsible of the different basement uplifts linked to the Carrizalito thrust between the Central and South cross-sections (see figure 12). In the hanging wall of the Carrizalito thrust, backthrusts are very common structures in all cross-sections; **b.** Perspective view of the three structural cross-sections showing the geometry of the basement-involved structures and its along-strike variations.

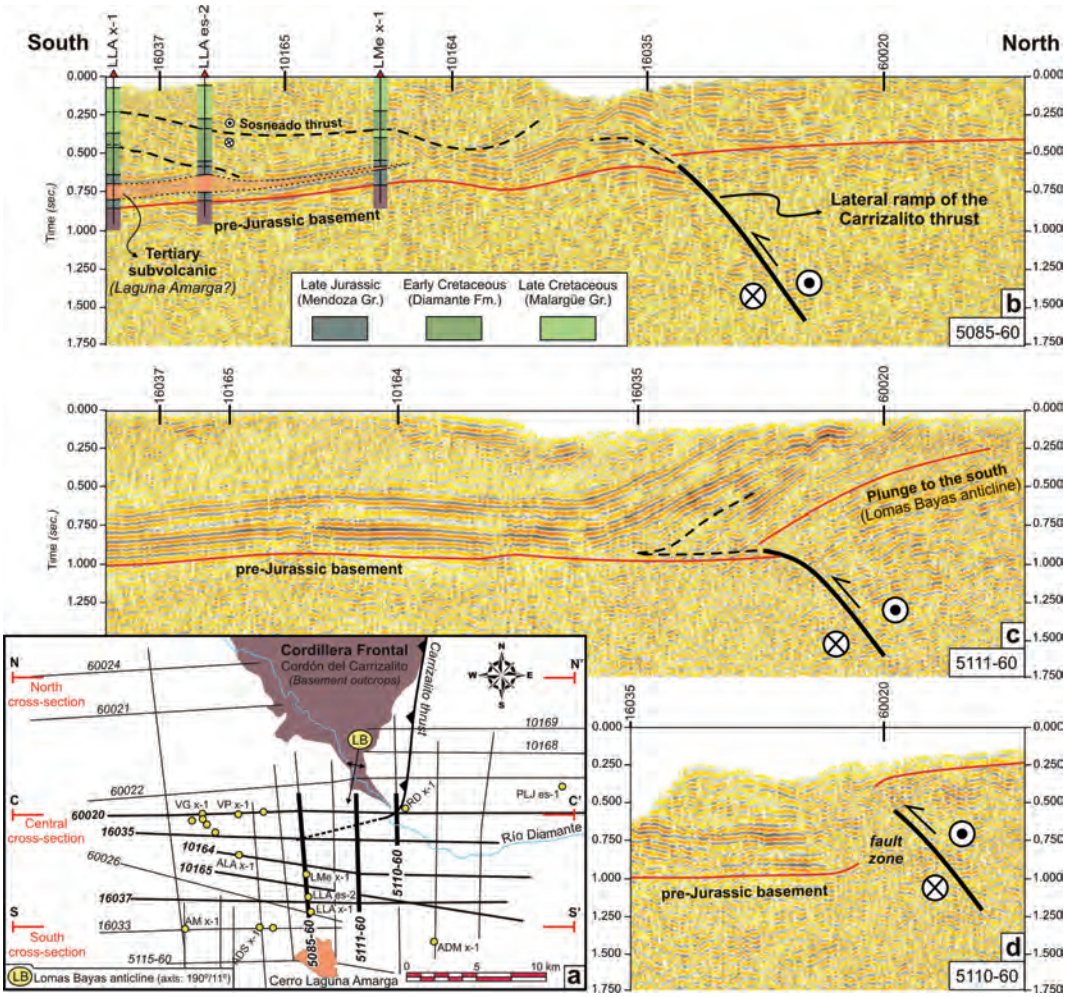

FIG. 12. **a.** Name and location of the seismic lines and oil wells considered for the construction of the balanced cross-sections; **b.-d.** Interpreted north-south seismic lines depicting the differential uplift of basement rocks between the Central and South cross-sections, related to a lateral ramp of the Carrizalito thrust. Displacement on this lateral ramp increases from west to east, which suggests a rotational or scissor movement along the fault.

and Davis, 2004, Galland *et al*., 2007a, Likerman *et al*., 2011). Specifically in the region of the Malargüe FTB, detailed measurements of minor faults support kinematic models that explain the Late Triassic-Early Jurassic extension (Bechis *et al*., 2010), while few contributions exists about such mesoscale structures in relation with the Andean compression (Cardozo *et al*., 2005; Turienzo *et al*., 2006). Fracture data at outcrop scale were collected by Turienzo (2008) during field works in the area of the Río Diamante and herein they are described and interpreted in order to understand its relationship with the major structures and the orientation of the associated regional stress field. The survey of fractures was made in 25 measurement sites or fracture stations (FS) evenly distributed in the entire region and from different geological units (Fig. 13). At each FS, we recorded fracture orientations and bedding plane attitudes and, where it was possible, we surveyed features indicating the mode of deformation (opening or shearing). The orientation data were plotted on equal-area (Schmidt) stereonets using the Georient 9.2 software. Most of the recognized fracture sets correspond to conjugate shear fractures, which according to Twiss and Moores (2007) are formed commonly previous or in the early stages of folding. Consequently, the fracture data were backtilted to its initial position by rotation along the strike of the bedding planes.

5.1. Fractures in cover rocks

Fracture stations (FS) 1 to 9 correspond to measurements made in Jurassic-Cretaceous sedimentary rocks across the thick- and thin-skinned sectors that form the Malargüe FTB in the Río Diamante area (Fig. 13). Fractures in FS 1 to 4 were measured in Cretaceous rocks exposed in the hangingwall of the Sosneado and Mesón thrusts. They show two dominant fracture sets, both striking ~N-S but dipping in opposite sense, which have a low angle respect to the bedding plane (Fig. 14a). These fractures have slickenside lineations on their surfaces, parallel to the dip direction of the fracture planes, indicating that shearing has occurred. They could be interpreted as conjugate shear fractures on the concave side of a folded layer (Fig. 14b). However, slickensides in the two fracture sets have steps that evidence a similar shear sense that allows to interpret them as *R* (Riedel) and *P* shear fractures generated in response to a general bedding-parallel shear affecting the sedimentary sequence (Fig. 14a). *R* and *P* fractures are secondary synthetic shears, having the same sense as the imposed shear (Hancock, 1985; Twiss

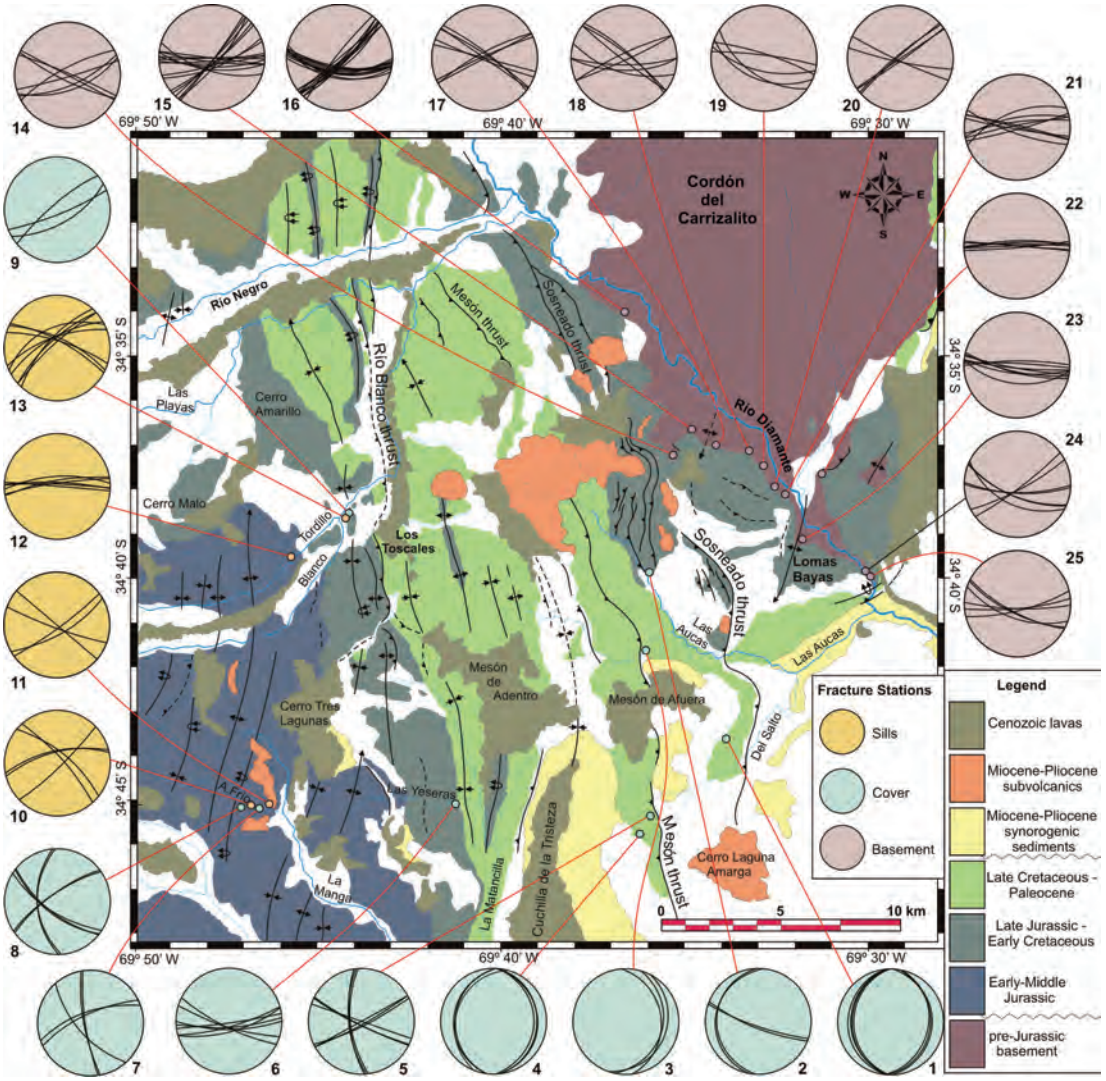

FIG. 13. Location of the fracture stations measured in basement, cover and subvolcanic rocks. In each plot, fracture data were backtilted to its initial position by rotation along the local strike of the bedding planes.

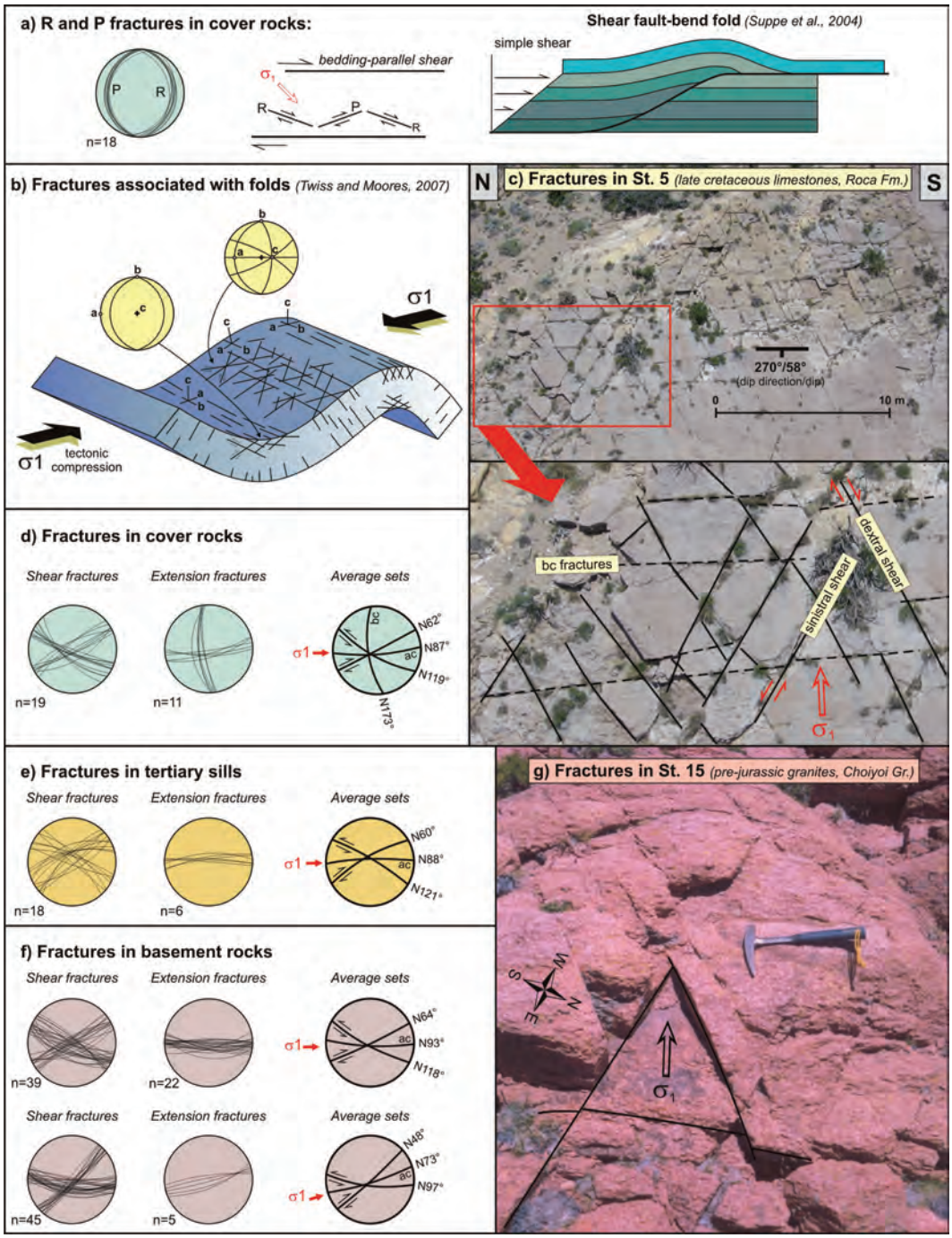

FIG. 14. Interpretation and examples of the fracture sets. **a.** *R* and *P* synthetic shear fractures at the hangingwall of the Mesón and Sosneado thrusts generated in response to bedding-parallel shear affecting the sedimentary sequence as occur in the shear fault-bend folds (Suppe *et al*., 2004); **b.** Main theoretical fracture sets formed in a folded layer (modified from Twiss and Moores, 2007); **c.** Photograph of fracture station 5, recorded on top of the Upper Cretaceous Roca Formation in the hangingwall of the Mesón thrust; **d, e, f.** Measurements in cover, subvolcanic and basement rocks respectively, with the average orientation of each fracture set and the estimated position of the maximum compressive stress (σ1); **g.** Photograph of fracture station 15, made in granites of Choiyoi Group.

and Moores, 2007), and they can be originated when layered rocks move along a thrust fault as per the shear fault-bend fold model (Suppe *et al*., 2004).

Four relatively steeply-dipping fracture sets are distinguishable in FS 5 to 9 affecting the different sedimentary units exposed in the studied area (Fig. 13). In the FS 5 the west-dipping limestones of the Roca Formation, uplifted and folded by the Mesón thrust, bear clearly three of these sets (Fig. 14c). A similar array of fractures is observed in the FS 8 affecting overturned beds of the El Freno Formation (Fig. 7b). The average orientation was calculated for each one of the four families of fractures recorded in cover rocks (Fig. 14d). Those fractures sets striking N62° and N119° show slickensides and offset relationships evidencing dextral and sinistral displacements respectively and consequently we interpreted them as conjugate shear fractures equivalent to those oblique sets developed in the limbs of a fold (Fig. 14b). The third set has a ~N-S strike, parallel to the strike of the strata and structures in this portion of the studied area, and it is almost perpendicular to the bedding. This set can be considered as *bc* extensional fractures, which are formed commonly during folding in the convex sides of folds (Hancock, 1985; Twiss and Moores, 2007). The fourth joint set was measured in the FS 6 and is composed of ~E-W striking open fractures, filled with calcite, which are interpreted as *ac* extensional fractures generated parallel to the direction of the maximum compressive stress (Fig. 14d). All the described fractures in Mesozoic sedimentary rocks are consistent with an E-W compression, which is in agreement with the overall N-S dominant trend of the South Central Andes (*e.g*., Ramos, 1988, 2009).

5.2. Fractures in Cenozoic sills

Outcrops of andesitic sills, with thicknesses between 1 and 3m, are particularly common in the western region of the studied area (Fig. 6a) where they are interbedded and folded with the sedimentary rocks (Fig. 7c). FS 10 to 12 were surveyed in sills intruding Early-Middle Jurassic rocks while the FS 13 is situated in andesites interbedded with Early Cretaceous rocks (Fig. 13). These rocks are affected by three families of subvertical joints striking at about N60°, N88° and N121° (Fig. 14e). The N88° set, which is considered as *ac* extensional fractures similar to the E-W joints in the cover rocks, is filled with calcite. This set bisects the dihedral angle of approximately 60° that is formed between the N60° and N121° sets which are interpreted as conjugate shear planes. These families of fractures are compatible with E-W shortening.

5.3. Fractures in basement rocks

The units that constitute the pre-Jurassic basement are well exposed along the Río Diamante and thus it was possible to measure numerous fractures that are represented in the FS 14 to 25 (Fig. 13). All stations in basement rocks were recorded near the basement-cover contact, which allow rotating the present-day data to its initial position considering the bedding attitude of the cover rocks. Analysis of the fracture pattern in the basement rocks is more difficult than in the cover units because they have suffered diverse tectonic events, particularly the Las Lagunitas Formation and the Tonalita Carrizalito (Fig. 3). For this reason the measurements were made exclusively in the Permian-Triassic granites and rhyolites of the Choiyoi Group, affected only by the Cenozoic Andean compression. Considering slight differences in the orientation of the fractures in basement rocks (Fig. 13), two different fracture patterns can be distinguished (Fig. 14f). The first array is composed of three subvertical fracture sets striking N64°, N93° and N118° (Fig. 14f, upper plots) resulting from measurements in FS 14, 17, 18, 19, 20, 22, 23, 24 and 25. The ~E-W set contains calcite-filled fractures interpreted as *ac* extensional fractures that bisect the other two sets, which show evidence of shearing and consequently they are considered conjugate shear planes. This fracture pattern is comparable to those observed in both sedimentary and subvolcanic rocks (Figs. 14d and 14e respectively) and agrees with an E-W direction of shortening. In a similar way, the second array of fractures is integrated by three fracture sets but in this case striking N48°, N73° and N97° (Fig. 14f, lower plots), recorded in the FS 15, 16 and 21 (Fig. 13). The N48° and N97° planes correspond to conjugate shear fractures as observed in the FS 15 (Fig. 14g), while the N73° set bisecting them is formed by open joints filled with calcite and is considered as *ac* extensional fractures. This different fracture pattern is compatible with a shortening direction striking ~N73°E (ENE-WSW).

6. Cenozoic structural evolution

It is widely accepted that the main compressive deformation in the Andes of central Argentina and Chile started in the Early-Middle Miocene (Charrier and Vicente, 1972; Ramos, 1988). Noticeable folds and faults affected the Eocene-Miocene volcanic sequences at the Chilean side of the Cordillera Principal (Fig. 5) from 22 Ma to 16 Ma (Charrier and Vicente, 1972; Godoy *et al*., 1999; Charrier *et al*., 2002; Farías *et al*., 2010). After ~16 Ma, contractional deformation migrated toward the east permitting the development of the Malargüe FTB and the uplift of the Cordillera Frontal in the Argentinean Andes essentially between the Middle Miocene and the Pliocene (Ramos, 1988; Baldauf, 1997; Combina and Nullo, 2005; Silvestro *et al*., 2005; Ramos and Kay, 2006; Giambiagi *et al*., 2008). The chronology of the Andean deformation has been exhaustively studied in the Aconcagua FTB (Giambiagi *et al*., 2003) and recently in the Malargüe FTB near the Río Atuel (Giambiagi *et al*., 2008) and the Río Grande valley (Silvestro and Atencio, 2009), to the north and south of the studied area respectively (Fig. 1b). Integrating the detailed geometrical reconstruction of the structures made by Turienzo (2008, 2010) with chronostratigraphic information of the Cenozoic strata (Kozlowski, 1984; Yrigoyen, 1993; Combina *et al*., 1993; Combina and Nullo, 1997, 2000, 2005, 2008, 2011) and $^{40}Ar/^{39}Ar$ dating of Cenozoic volcanic and subvolcanic rocks (Baldauf *et al*., 1992; Baldauf, 1997, Nullo *et al*., 2002; Giambiagi *et al*., 2008), we propose a kinematic model in order to elucidate the structural evolution during the Cenozoic Andean orogeny in the region of the Río Diamante (Fig. 15). Sequential reconstruction of the structures is based in the Central cross-section (Fig. 4b) because it is the best constrained by both surface and geophysical data and it shows clearly different structural domains that involve thin-skinned and thick-skinned deformation. The proposed structural evolution (Fig. 15) encompasses from the Middle Miocene (14.5 Ma) to the Middle Pleistocene (0.5 Ma), which is in agreement with the evolution of synorogenic basins in the south of Mendoza between 16 and 1 Ma (Silvestro *et al*., 2005) and the evolution of structures in the Río Atuel area from 15 to 1 Ma (Giambiagi *et al*., 2008).

6.1. Deformation stage 1 (14.5 - 10.8 Ma)

The restored Central cross-section illustrates the Mesozoic sedimentary sequence progressively onlapping toward the foreland, in a stage previous to the Andean deformation (Fig. 15a). Numerous andesitic sills are situated concordantly into the Early-Middle Jurassic strata (Fig. 6a), in front of the westernmost basement-involved structures (Fig. 7). These subvolcanic rocks were intruded before the beginning of our deformation sequence and then were folded together with the sedimentary rocks, since they have the same attitude than the sedimentary beds and are affected by comparable fracture sets (Figs. 14d and 14e). Few kilometers toward the south, in the north border of the Río Atuel (Fig. 1c), pre-tectonic subvolcanic rocks folded together with the Early Jurassic strata have an age of 14.48±0.61 Ma (Giambiagi *et al*., 2008). Based on the similarities and proximity of these rocks it is possible to consider this value of ~14.5 Ma as a maximum age for the beginning of the compressive deformation responsible of the structures here analyzed. In the context of our interpretation the oldest structure is the thrust that generated the basement wedge 1, with the Cerro Malo folds (1) and Arroyo Tordillo backthrusts (2) in its hangingwall (Fig. 15b). This wedge was inserted in Early-Middle Jurassic sedimentary rocks, transmitting displacement along the evaporites of Tábanos Formation to produce the Río Blanco anticline (7) in the cover. Close to the union between the Arroyo Frío and the Arroyo La Manga (Fig. 6a), subvolcanic rocks are disposed unconformably above overturned Jurassic beds and intensely folded sills (Figs. 7a and 7c) and clearly post-date the deformation event responsible of such structures. The Cerro Chivato is a subvolcanic body with associated dykes emplaced in Jurassic rocks southward of the Río Atuel (Fig. 1c), which according to Baldauf (1997) is post-tectonic and has an age of 13.94±0.08 Ma. The Cerro Chivato and the Arroyo Frío subvolcanic rocks can be correlated since they have a similar structural relationship postdating the folding of the Jurassic strata and they are located aligned parallel to the same structural trend. Despite of uncertainties and small differences in age of pre and post-tectonic subvolcanic rocks, a first pulse of deformation can be constrained in the studied area between 14.5 and 14 Ma (Fig. 15b).

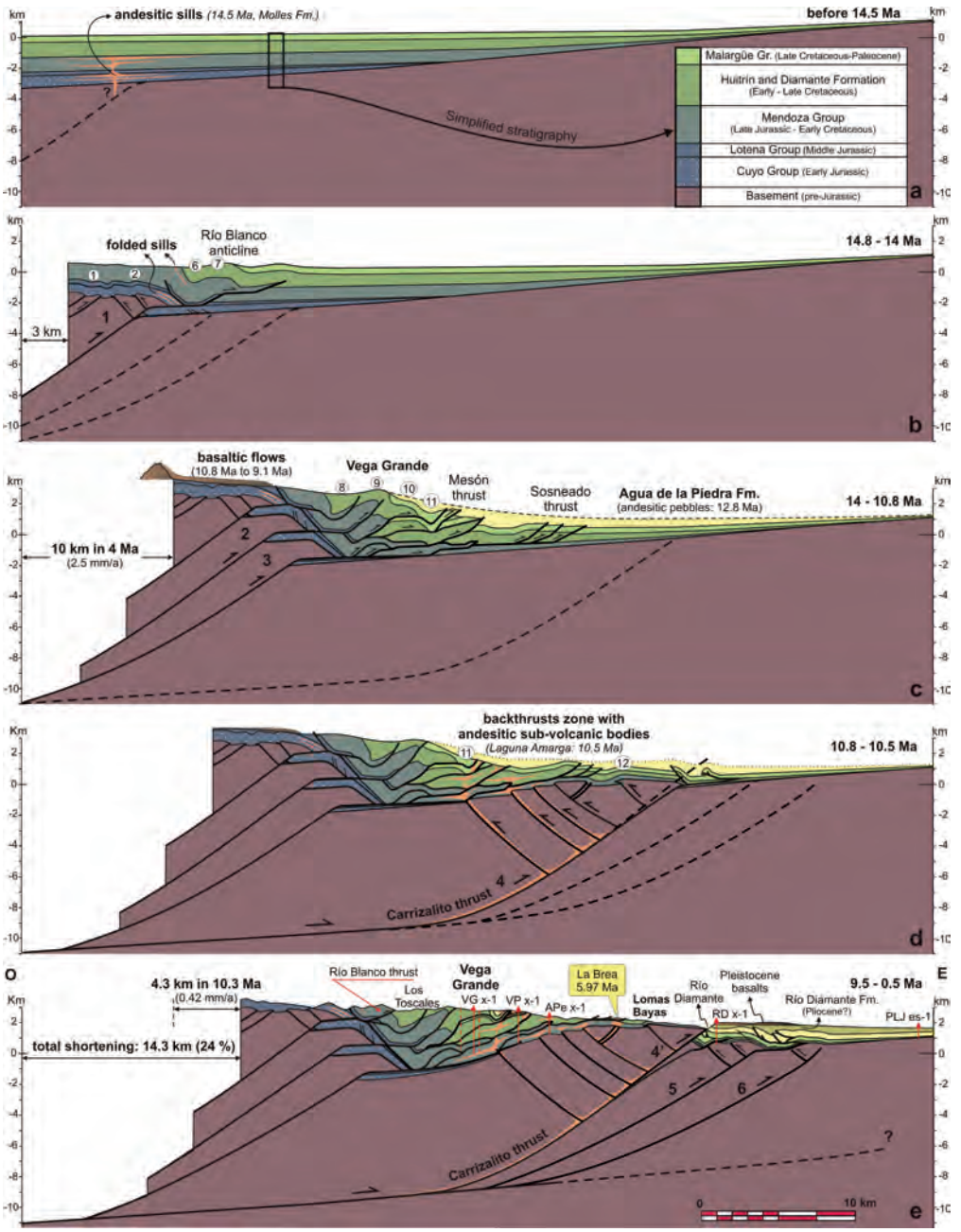

FIG. 15. Sequential structural evolution proposed for the Malargüe FTB and the Cordillera Frontal at the Río Diamante area, based on the Central cross-section. **a.** Intrusion of andesitic sills in the undeformed sedimentary sequence; **b.** The basement wedge 1 folded Jurassic strata and andesitic sills and generated the Río Blanco anticline; **c.** Development of basement wedges 2 and 3 created the important structural relief at the western sector, covered by horizontal basaltic flows (10.8 Ma), and formed the thin-skinned structures in the central sector including the easternmost Sosneado thrust, previous to the intrusion of the Laguna Amarga andesites (10.5 Ma); **d.** Faulting progressed toward the foreland with the formation of the Carrizalito thrust and its related backthrust system. These structures could have controlled the eastward expansion of arc magmatism and the emplacement of several subvolcanic bodies (10.5 to 5.5 Ma) in the region of backthrusting; **e.** A branch of the Carrizalito thrust produced the Late Miocene uplift of basement rocks at the southern Cordillera Frontal. Development of the basement-involved structures 4 and 5 in depth deformed the overlaying Pliocene-Pleistocene sediments which are covered by unfolded Middle Pleistocene basalts. Structural development of the western and central sectors imply a shortening rate of ~2.7mm/a, considerably higher than the 0.42 mm/a in the eastern sector.

Subvolcanic rocks that form the Cerro Laguna Amarga (10.56±0.04 Ma) are located over the fault trace of the Sosneado thrust (Fig. 2) and according to Baldauf (1997), they were not affected by this fault. The Sosneado thrust is the easternmost structure of the thin-skinned sector of the Malargüe FTB (Fig. 4) and according to Turienzo (2010), structures in the cover are genetically linked to the thick-skinned structures developed to the west (Fig. 15c). Thus, all these structures should be older than 10.5 Ma. Moreover, subhorizontal basalts of the Cerro Tres Lagunas (9.07±0.24 Ma), Cerro Malo (10.32±1.44 Ma) and Cerro Tordilla (10.84±0.52 Ma) are post-tectonic volcanic rocks (Giambiagi *et al*., 2008) that cover the folded Jurassic rocks in the western sector (Fig. 2). Taking into account the oldest age of these post-tectonics rocks, the final emplacement of the basement wedges in the western sector and consequently the complete development of the folds and thrusts in the thin-skinned sector of the Malargüe FTB can be constrained between 14 and 10.8 Ma (Fig. 15c). As in the first basement wedge, the main thrust associated to the second wedge transferred displacement over the Early-Middle Jurassic rocks generating several folds and thrusts as the Vega de los Patos anticline (9) and the repetitions of the Cretaceous units in the Vega Grande oil field (Fig. 9). Furthermore, these repetitions of the Mesozoic levels produced the movement along the Mesón thrust which put Late Cretaceous over Miocene rocks (Figs. 8c-d and 15c). The third basement wedge is interpreted moving toward the east along the evaporites of the Jurassic Auquilco Formation. The displacement associated with this wedge originated duplex structures involving the Late Jurassic-Early Cretaceous rocks and furthermore, following a flat-ramp-flat trajectory, it produced faulting associated to the Sosneado thrust (Fig. 15c).

The sequential reconstruction of the structures across the thick and thin-skinned sectors of the Malargüe FTB during this first deformational stage depicts a normal (piggyback) sequence of faulting (Figs. 15a-c). Our model of basement wedges or basement-cored fault-bend folds at the thick-skinned sector of this segment of the Malargüe FTB, each one transmitting displacement to the cover generating most of the thin-skinned structures (Figs. 4, 9 and 15a-c), can be compared with the uncoupled model of basement-cover interaction related to a high propagation to slip ratio (p/s) proposed for the southern Malargüe FTB (Giambiagi *et al*., 2009).

It is important to emphasize that magmatic activity occurred during this stage of deformation, as demonstrated by andesitic boulders of 13.44±0.08 Ma and 12.83±0.1 Ma (Baldauf, 1997) at the base of Agua de la Piedra Formation. Layers of this unit are folded constituting both flanks of the Cuchilla de la Tristeza syncline (11) and they were transported toward the east above the Mesón and Sosneado thrusts, which were mainly active previous to the intrusions of the Cerro Laguna Amarga (Baldauf, 1997). Syntectonic accumulation of the Agua de la Piedra Formation in the studied area can be confined to the Middle-Late Miocene, approximately between 12.83 and 10.56 Ma, and the diachronic character of this unit proposed by Combina and Nullo (2008, 2011) explains the differences in age with respect to other sectors of the Malargüe FTB.

6.2. Deformation stage 2 (10.8-0.5 Ma)

Several subvolcanic rocks of the Huincán Eruptive Cycle as the Cerro Laguna Amarga (10.56±0.04 Ma), Cerro La Brea (5.97±0.08 Ma), Cerro Media Luna (6.52±0.04 Ma) and Cerro Mala Dormida (5.58±0.07 Ma), are aligned along the Sosneado thrust (Fig. 2). According to Baldauf (1997), these intrusive rocks were emplaced after the activity of the Sosneado thrust and along the zones of crustal weakness created by this fault. Analyzing more rigorously the distribution of these subvolcanic rocks, including those detected by the exploration wells, it results that these rocks are situated in a broader zone coincident with the area of backthrusting in the Carrizalito thrust hangingwall (Fig. 11a). All oil wells located above these structures in the Central and South cross-sections show that subvolcanic rocks are intruding the Late Jurassic-Early Cretaceous rocks below the decollement of the Sosneado thrust (Figs. 4b and 4c), supporting the hypothesis of deeper channels for the source of magmas. For these reasons, we consider that these Neogene intrusives were emplaced through the backthrusts in the hangingwall of the Carrizalito thrust (Fig. 15d), as we discuss in the section 7.2. It constrains the minimum age for the backthrust, if they were formed previously or simultaneously to the intrusion of the subvolcanic rocks, to 10.56 Ma or older in the south and 5.58 Ma or older in the

north. This variability in the age of the subvolcanic rocks from south to north allows us to evaluate two hypotheses. In the first one the backthrusts have the same age in the whole region, approximately 10.5 Ma or a slightly older, and the magmatism has varied temporally and spatially producing younger intrusions toward the north (5.5 Ma). In the second interpretation, the intrusions and the backthrusts are contemporaneous and they progressed together from the south to the north. We do not have yet strong evidence to support one over other hypothesis.

In our evolutionary model, after the structural development of the thick and thin-skinned sectors of the Malargüe FTB, a noticeable difference in structural relief was created between the western and the eastern regions of the studied area (Fig. 15c). Considering conceptually the model of the Coulomb critical wedge (Davis *et al*., 1983), this differential height and the consequent abrupt topographic slope produced a supercritical wedge favoring the formation of new structures toward the foreland in order to attain a critical taper. This model allows us to understand the generation several kilometers eastward into the foreland of the west-dipping Carrizalito fault (Fig. 15d). The absence of efficient detachment horizons related to lithological changes of the sedimentary rocks in this portion of the basin precludes the development of large basement wedges as in the western sector and instead a significant deformation occurred by backthrusting in the hangingwall of the Carrizalito thrust. Structures associated to backthrusts in basement rocks are exposed in the Central cross-section and they are in depth in the South cross-section (Fig. 4), as we described in the section 4.1.3, due to an ENE lateral ramp that accommodate the different displacement of the Carrizalito thrust between the north and the south (Fig. 11). This suggests that backthrusts, including associated folds as the Lomas Bayas anticline, were not originated as classical pop up structures due to a major displacement along the Carrizalito thrust in the north. On the contrary, we consider that backthrusts formed at the north and south in an early stage, when the forward movement along the Carrizalito thrust was hindered (Fig. 15d), and then these structures were uplifted in the northern area because the along-strike differential slip of the thrust.

Continued compression caused a branch of the Carrizalito thrust to place pre-Jurassic basement rocks over the Cenozoic syntectonic rocks, as seen in the North and Central cross-sections (Fig. 4). Strata of the Loma Fiera Formation lie unconformably over the Agua de la Piedra Formation in the Cuchilla de la Tristeza syncline and contain granite pebbles (Combina and Nullo, 2000), Permian-Triassic volcanites of ~220 Ma and pumice clasts of 9.51±0.07 Ma (Baldauf, 1997), indicating that basement rocks were already exposed by the Late Miocene. Unfortunately there are not enough data to constrain accurately the age limit of this uplift. On the other hand, it is clear that the vertical offset of approximately 1 km due to the displacement produced by the Carrizalito thrust (Fig. 15e) took place before the basalts extruded in the north side of the Río Diamante (Fig. 10c). Recent studies that analyze the Quaternary geomorphological evolution of the Río Diamante valley (Baker *et al*., 2009) conclude that these basalts were contemporaneous with the extrusion of Middle Pleistocene ignimbrites (~0.5 Ma). Despite of the uncertainties about the age of the basement uplift that formed the Cordón del Carrizalito, it is possible to assume its occurrence in the Late Miocene previously or simultaneously to the accumulation of the Loma Fiera Formation. This assumption is in agreement with the progressive development of the Cordillera Frontal from north to south, finishing with the uplift of its southern end during the Late Miocene-Pliocene (Giambiagi *et al*., 2003). New basement-involved structures that folded slightly the overlying sedimentary rocks were formed eastward of the Carrizalito thrust, as the Del Medio anticline in the South cross-section (Fig. 4c). In the Central cross-section the thrust number 5 produced the elevation of the basement with respect to its regional position as can be seen in the YPF.RD.x-1 well (Fig. 15e), folding the Miocene strata of Agua de la Piedra Formation which locally are affected by a backthrust (Fig. 10f). The Late Miocene-Pliocene strata of the Río Diamante Formation are gently folded by this west-vergent structure and they are covered by horizontal Middle Pleistocene basalts (Fig. 10c). In the same region, Baker *et al*. (2009) reported folding of Early-Middle Pleistocene sediments that is the surface expression of a blind thrust verging to the west. Thus, the deformation of the easternmost part of the studied region, that originated basement-involved structures in depth and affected Miocene to Pleistocene sediments in surface (Fig. 15e), probably occurred between the Pliocene and the Middle Pleistocene.

Thick-skinned deformation in the eastern sector of the study area occurred in a different mode than in the western sector since the stratigraphic pile lacks sedimentary rocks that can behave as efficient detachment horizons, which in turn precludes the development of basement wedges with large displacements. The west dipping Carrizalito thrust initially remained as a blind thrust that generated negligible deformation toward the foreland and significant deformation occurred by backthrusting in its hangingwall (Fig. 15d), while further compression produced a branch of the thrust that propagated toward the surface forming a trishear fault propagation fold in the overlying strata (Figs. 10d and 15e). This style of deformation in the southern part of the Cordillera Frontal can be compared with the coupled model of basement-cover interaction, related to a low propagation to slip ratio (p/s), which characterizes the external thick-skinned structures in other segments of the Malargüe FTB (Giambiagi *et al*., 2009).

6.3. Quaternary tectonic activity

Despite that the main period of mountain building during the Andean orogeny at this latitude can be constrained between the Middle Miocene and the Middle Pleistocene, there are widespread evidences of neotectonic activity demonstrating Quaternary to recent compression (Polanski, 1963; Cortés *et al*., 1999). This is notoriously illustrated in the Río Diamante where the Middle Pleistocene basalt flow forms a monocline structure, with ~25 m of vertical offset (Baker *et al*., 2009), in front of the Carrizalito thrust (Fig. 10c). Further south of the studied area, the Mesón thrust repeated the Loma Fiera Formation (Volkheimer, 1978; Kozlowski, 1984) evidencing that its activity outlasted the Late Miocene while the Sosneado thrust placed Late Cretaceous-Paleocene rocks on top of Pleistocene fanglomerates and it is covered by Holocene deposits (Giambiagi *et al.*, 2008). Even though the subvolcanic rocks of the Cerro Laguna Amarga (10.56 Ma) were not affected by the Sosneado thrust (Baldauf, 1997), the Quaternary reactivation of this fault in the surrounding areas can be explained considering that the thrust was split by the rigid, pre-existent intrusive into branches along its margins (Giambiagi *et al.*, 2008).

The present day convergence between the Nazca and South America plates generates an intense seismicity along the Andes, particularly in the flat-slab segment of subduction (Fig. 1b), producing numerous earthquakes (Barazangi and Isacks, 1976; Cahill and Isacks, 1992). Operating a portable broadband seismic network as part of the Chile-Argentina Geophysical Experiment (CHARGE), Alvarado *et al*. (2005) have studied crustal earthquakes that occurred in the back arc and under the main cordillera in the south-central Andes obtaining focal mechanisms and source depths using the moment tensor inversion method. A moderate-sized earthquake occurred in the studied area few kilometers southward of the South cross-section (Fig. 11a). The focal mechanism solution for this quake indicates a shallower west-dipping or a more inclined east dipping fault plane with dip-slip movement and a very shallow focal depth of 3 km (Alvarado *et al*., 2005). In the context of our structural interpretation, this focal solution reveals the current tectonic activity on the Carrizalito fault or alternatively along any of its associated backthrusts (Fig. 11b). Neotectonic movement on this fault system can be accounted for by considering again the model of the Coulomb critical wedge (Davis *et al*., 1983), since in the southern region the basement-involved structures are notably more evolved in the west than in the east (Fig. 4c) favoring the subsequent structural development in the foreland. On the other hand, in the north region, there are large thick-skinned structures exposed in the eastern sector that build a subcritical wedge (Fig. 4a). Thus, deformation is expected to be concentrated in the western sector by means of out-of-sequence faults as the Río Blanco thrust (Fig. 15e) and other similar structures described in the north segment of the Malargüe FTB westward of the Cordillera Frontal (Broens and Pereyra, 2005; Kim *et al*., 2005, Fuentes and Ramos, 2008). Active faults also have been described in the western Andean mountain front of Chile, represented by the west-vergent San Ramón fault (Armijo *et al*., 2010). Strike-slip deformation is presently reported in the axial zone of the cordillera by seismic activity in earthquakes M>5, which would be related to the opposition of shortening exerted by the high elevation reached by the mountain belt in the Pliocene (Farías *et al*., 2010). The presence of active faults along the east and west margins of the Cordillera suggests that the Andes at this latitude are currently growing as a double-vergent orogen (Fig. 5).

7. Discussion

7.1. Shortening rates and comparison with GPS and plate tectonics data

Shortening estimates from the interpreted cross-sections combined with the temporal constraint of deformation in different sectors allow us to calculate the respective shortening rates across the Malargüe FTB and the Cordillera Frontal in the Río Diamante area. Taking into account that the shortening in the studied area is in the order of 14 km (Fig. 4) and that the main deformation producing the observed structures occurred between 14.5 and 0.5 Ma (Fig. 15), we determined an average shortening rate of 1 mm/a. However, this value is a long-term average calculated over millions of years and thus it is difficult to compare with short-term geodetic rates averaged over only a few years. Following our sequential reconstruction of structures in the Río Diamante area, it is clear that substantial differences exist between the western and the eastern sectors with respect to the structural style, the amount of shortening and the timing of deformation (Fig. 15). Development of basement wedges in the western sector responsible of the formation of structures in the thin-skinned sector of the Malargüe FTB produced ~10 km of shortening between 14.5 and 10.8 Ma (Fig. 15c), resulting a rate of shortening of 2.7 mm/a, which represents an important Middle Miocene compressive period. Measured shortening in the eastern sector of the Central cross-section, due to the development of the Carrizalito thrust, its associated backthrust system and the easternmost basement-involved structures, is 4.3 km (Fig. 15e). This structures were formed from 10.8 to 0.5 Ma and consequently the rate of shortening is 0.42 mm/a, substantially less than those of the western and central sectors, which suggests that Andean contraction slowed down from the Late Miocene to the Middle Pleistocene. Our estimated shortening rates of 0.42 and 2.7 mm/a are strongly consistent with the strain rates calculated in the southern segment of the Malargüe FTB, ranging from 0.5 to 2.6 mm/a (Giambiagi *et al*., 2009). These authors determined that structures evidencing low and high strain rates can be related to low and high propagation to slip values (p/s) respectively of the fault-related folds, suggesting a close relation between strain rates and fault-fold mechanisms. In the Chilean side of the Andes, Armijo *et al.* (2010) determined that the west-vergent San Ramon fault has a long-term average slip rate of ~0.25-0.3 mm/a considering 4-5 km of displacement in 16 Myr, although based on morphological and thermochronological data Farías *et al*., (2010) suggest that this slip is slightly overestimated. Anyway, this magnitude of deformation related to the Chilean structures is comparable with our estimations in the Argentinean side.

Space geodetic estimates of the rate of Nazca-South America convergence averaged over several years show that present day rates are significantly slower than the 3 million year average NUVEL-1A model (Norabuena *et al*., 1999). We use the UNAVCO Plate Motion Calculator (http://sps.unavco.org/crustal_motion/dxdt/nnrcalc/) to evaluate the convergence rate between the Nazca plate and an arbitrary point within the studied area (34°40'S - 69°45'W) using several geodetic models and the geological Nuvel-1A model. The averaged present day convergence rate at this latitude calculated from five geodetic models is ~70 mm/a in the direction N77°E (Fig. 1a), while from the Nuvel-1A model the convergence rate is ~80 mm/a in the same direction. Pardo Casas and Molnar (1987) used plate reconstructions based on the age and position of magnetic anomalies to evaluate the relative motion between the Nazca and South American plates, demonstrating that the rate of convergence has not been constant. Convergence was rapid between 50 and 40 Ma (~150 mm/a), becomes slow from 36 to 26 Ma (35-50 mm/a), and has been again fast since 26 Ma (110-112 mm/a) including, though with uncertainties, a faster convergence between 20 and 10 Ma than for 10-5 Ma (Pardo Casas and Molnar, 1987). According to these authors, the periods of rapid convergence correlate remarkably well with the main phases of deformation in the Peruvian Andes, which obviously implies that the tectonic activity of the overriding plate at subduction zones is strongly dependent on the convergence rate. Using seafloor data and the geomagnetic time scale for the Cenozoic, Somoza (1998) analyzed the Nazca-South America relative motions and determined the paleoconvergence direction at several points near the present plate boundary zone. At 30°S the results suggest that a regime of relatively high convergence rate was sustained between 20 and 11 Ma (130-110 mm/a) and an abrupt decrease in convergence velocity occurred between 11 and 5 Ma (78 mm/a). The convergence direction was roughly

E-W during the Late Oligocene-Early Miocene and then it becomes slightly oblique (Somoza, 1998), up to the N77°E present day azimuth (Fig. 1a). These small variations in the convergence direction allow us to elucidate the stress field responsible of the mesoscale structures surveyed in the Río Diamante area. The former direction explain most of the measured fracture sets in the studied area, related to E-W shortening, while the younger oblique convergence direction could have produced the family of fractures affecting the basement rocks in the eastern sector related to WSW shortening (Fig. 14f).

Studies based on GPS geodesy in the South-Central Andes show that while the Nazca-South America current convergence rate is ~70 mm/a, the coastal GPS stations move towards the stable craton at rates of 30-40 mm/a and stations in the backarc move towards the craton at a third of this rate, or even more slowly (Kendrick *et al*., 2006). The results of these authors suggest that active deformation in the backarc is focused on a narrow zone (< ~50 km wide) near the backarc thrust frontal zone, which is consistent with a rigid Andean block or 'microplate' overthrusting the South American craton at rates on the order of ~3-6 mm/a. At the latitude of the Malargüe FTB, this block is currently moving nearly parallel to the strike of the orogen with a total predicted horizontal velocity magnitude of ~1.6 mm/a, while the trench perpendicular component is about 0.6 mm/a (Kendrick *et al*., 2006). Despite that the maximum velocities related to backarc strain are less than a few mm/a, which approach to the resolution of the technique itself, we found that our shortening rates (0.42-2.7 mm/a) calculated from balanced cross-sections fall within the same order of magnitude as these GPS estimations.

7.2 Relationship between Cenozoic magmatism and Andean tectonics

There is a close and complex relationship between the tectonic evolution of the Andes during the Cenozoic and the coeval magmatic activity. Important differences along strike are apparently related to the geometry of the subducting plate, as well as to variations in crustal rheologies and changes in the trench roll-back velocity through time (Jordan *et al*., 1983; Ramos and Kay, 2006; Ramos, 2009). The active Andean Southern Volcanic Zone arc front is located near the Chilean-Argentine border, to the south of 33.5°S (Jordan *et al*., 1983; Ramos *et al*., 2002). Andesites of the Huincán Eruptive Cycle exposed in the studied area represent an expansion of the arc magmatism toward the foreland, beyond the narrow confines of the modern magmatic arc located at the crest of the Cordillera Principal (Baldauf, 1997). Older Huincán andesites as the Cerro Chivato (~14 Ma) situated at the western sector and younger subvolcanic rocks as those exposed from the Cerro Laguna Amarga to Cerro Mala Dormida (10.5 to 5.5 Ma), located ~20 km eastward, indicate a foreland expansion of the magmatic arc between Middle and Late Miocene (Baldauf, 1997). As we mentioned before, Baldauf (1997) considered that the younger subvolcanic rocks were intruded along the Sosneado thrust during the waning phases of the Malargüe FTB deformation. However, we have described sills in several oil-wells surrounding the Cerro Laguna Amarga and intruding the Late Jurassic-Early Cretaceous rocks below the Sosneado thrust (Fig. 4), which suggest the existence of deeper channels for the source of magmas. Location of these subvolcanic rocks in the region of backthrust affecting the Carrizalito thrust hangingwall (Fig. 11a), allows us to interpret them as emplaced through such fault system (Fig. 15d). In the region of Bardas Blancas, southward of the studied area (Fig. 1b), the Cenozoic subvolcanic body of the Cerro Palao Mahuida is placed over the fault trace of an exposed basement-involved backthrust and it was interpreted as emplaced using this fault as a channelway and under a compressive stress field (Dimieri, 1992b). More recently, many examples of Neogene-Quaternary magmatism developed under compressional tectonic settings and commonly on top of thick-skinned structures were documented along the Andes (Tibaldi, 2005; Galland *et al*., 2007a; González *et al*., 2009). Experimental modelling, performed in order to envisage the interaction of magmatism and tectonics in the Andes, that depicts simultaneous magmatic injection and shortening into a deforming brittle crust, show that the magma forms a basal sill and then typically rises along a thrust fault whereas if the injection outlast shortening the magma rises along backthrusts (Galland *et al*., 2007b). In these experiments thrust faults provided conduits for fluid so reaching the surface and once in place, the fluid and the soft basal sill act as detachments controlling the pattern of subsequent deformation (Galland *et al*., 2007b). This feedback between faulting and magmatism is also supported by field evidences

in regions where melt-enhanced deformation is an important mechanism (Hollister and Crawford, 1986). Magma can be stored as subhorizontal sills migrating horizontally large distances, in the order of kilometers, along flat segments of thrusts and it may be extruded through ramps (Galland *et al*., 2007a, 2007b; González *et al*., 2009). These mechanisms provide an explanation to the foreland expansion of the Huincán subvolcanic rocks considering a lateral migration of the magma along the flat portion of an incipient Carrizalito thrust and subsequent rising through the backthrusts formed in the hangingwall of this structure (Fig. 15d). Moreover, the accumulation of melt facilitates further deformation and thus increasing the displacement along the Carrizalito fault that leads to the break-through of basement rocks thrusting it over younger sediments (Fig. 15e). Magmatic activity was intense during the Miocene and Pliocene in Chile, where widespread volcanic and plutonic rocks are exposed approximately between 33º and 35ºS (Maksaev *et al*., 2003; Deckart *et al*., 2010; Piquer *et al*., 2010). Fission track analysis in apatite reveal cooling ages from 21 to 3.1 Ma and suggest an important period of Andean uplift and denudation between 5.6 and 3.1 Ma (Maksaev *et al*., 2003). Piquer *et al*. (2010) dated a granodiorite at 7.8±0.4 Ma (K-Ar in biotite) and interpreted the emplacement of intrusives rocks as being controlled by the Infiernillo-Los Cipreses fault system, a set of Late Eocene-Middle Miocene normal faults that acted as reverse faults during an episode of major tectonic contraction in the Late Miocene, which induced the ascent of the intrusive bodies. Barren Miocene granitoids located between 33º and 34ºS, with arc-like signature and crystallization ages from 14.9±0.2 Ma to 10.2±0.2 Ma (U-Pb LA-ICPMS), suggest that in this region magmatism does not reflect eastward arc front migration (Deckart *et al*., 2010).

Volcanic rocks in the Sierra de Chachahuén, south of Mendoza province (Fig. 1b), have an arc-like magmatic signature and range in age from 7.2 to 4.8 Ma (Kay *et al*., 2006). This volcanic field located about 500 km to the east of the modern trench is interpreted as an important foreland shifting of the arc magmatism that is associated with contractional deformation in the Malargüe FTB between 15 and 5 Ma and with the Late Miocene uplift of the San Rafael block in central Mendoza (Ramos and Kay, 2006). This evidence suggests a Middle-Late Miocene period of transient shallow subduction that reached its climax near 5 Ma, followed by a Pliocene-Pleistocene episode of steepening of the Benioff zone producing widespread eruption of intraplate alkaline magmas in the Payenia igneous province and finally a Late Quaternary shallowing of the subduction zone responsible of the neotectonic activity in the San Rafael block (Kay *et al*., 2006; Ramos and Kay, 2006). Galarza *et al*. (2009) analyzed the structural development in the southern segment of the Malargüe FTB, considering the variations in the angle of the Benioff zone proposed by Kay *et al*. (2006) as a primary factor controlling the tectonic evolution. Following these authors we analyze how suitable is the model that considers changes in the angle of subduction to explain the structural development of the Malargüe FTB and the Cordillera Frontal in the Río Diamante area. Based in our structural evolution for the studied region of the Andes (Fig. 15) we calculate that the maximum shortening rate occurred in the Middle Miocene, from ~15 to 11 Ma, but important contraction can be extended to the Late Miocene considering that the basement rocks in the eastern sector were uplifted contemporaneously with the deposition of the Loma Fiera Formation. This stage of high compressive deformation fits well with the model of Middle-Late Miocene flat-slab in the southern Mendoza (Kay *et al*., 2006; Ramos and Kay, 2006). The noticeable diminution of the shortening rate after the Late Miocene suggests a period of low contractional strain, perhaps reflecting a steepening of the subduction zone, but at the present no evidence of significant extensional tectonics have been found in this region. Further studies focusing on age and tectonic conditions under which the Río Diamante Formation was deposited, may shed some light about this deformation stage. The available data suggest that the upper sections of this unit have Pliocene age and it may have experienced intraformational unconformities related to compressive deformation (Combina and Nullo, 1997, 2005, 2011). Another way to explain the diminution of shortening rate during the Neogene, other than slab steepening, is to consider the high elevation reached by the mountain belt in the Pliocene that would not differ too much from its current elevation, which generated a large vertical stress enough to prevent contraction within the orogen (Farías *et al*., 2008; 2010). However we consider that the decreasing convergence rate between the Nazca and South American plates, already

discussed in section 7.1, is the strongest argument supporting such shortening changes.

Finally, widespread evidences of Quaternary compressive deformation are well documented in the studied area, including recent seismic records of shallow quakes possibly related to the Carrizalito fault system at depth. These features could be associated to another younger shallowing of the subducted plate proposed for southern Mendoza by Ramos and Kay (2006), although they suggest that the present day reactivated mountain front is located far into the foreland, in the eastern slope of the San Rafael block. As we mentioned in sections 6.2 and 6.3, recent activity along the Carrizalito fault system could be related to a supercritical wedge geometry of the FTB, since in the southern region the basement-involved structures are notably more evolved in the west than in the east (Fig. 4c) favoring the subsequent structural development in the foreland.

8. Conclusions

A thorough study of the structures in the Argentinean side of the Andes at 34°40'S allows us to establish a kinematic model that reveals the structural evolution of this portion of the Andean belt. Based on the integration of balanced structural cross-sections with previous studies of Cenozoic synorogenic rocks and $^{40}Ar/^{39}Ar$ ages of coeval volcanic and subvolcanic rocks, we propose that the development of the thick-skinned Malargüe fold-and-thrust belt and the easternmost basement uplift of the Cordillera Frontal occurred between the Middle Miocene and Middle Pleistocene. Andean deformation in the Río Diamante area begun around 14.5 Ma with the growth of thick-skinned structures at the western region of the Malargüe FTB, formed by large basement wedges that propagated along detachment horizons within the cover generating thin-skinned structures. Stacking of three basement wedges, related to Andean thrusts rooted at ~10 km within the basement, explains the high structural relief of basement rocks together with large horizontal shortenings in cover rocks observed in this segment of the Malargüe FTB. The development of these genetically linked thick and thin-skinned structures finished with the insertion of the third basement wedge and its associated deformation in cover rocks along the Sosneado thrust, whose main displacement occurred before the extrusion of 10.8 Ma volcanic rocks. These structures imply ~10 km of shortening, representing an important Middle Miocene compressive period (2.7 mm/a). Systems of fractures measured in basement, cover and subvolcanic rocks indicate an E-W direction of compression. The high structural relief attained after the Middle Miocene deformation created a supercritical Coulomb wedge and thus faulting progressed toward the foreland by means of the west-dipping, Carrizalito thrust. At the eastern sector, the lack of efficient detachment horizons within the cover rocks difficulted the development of large basement wedges as in the west and instead a significant deformation occurred by backthrusting in the hangingwall of the Carrizalito thrust. Widespread subvolcanic rocks (10.5 to 5.5 Ma) with arc-like signature, exposed in the region of the backthrusts, suggest a close relationship between the arc magmatism and this antithetic fault system. These igneous rocks could reflect an expansion of the arc magmatism toward the east, since coeval Miocene-Pliocene volcanic arc rocks emplaced during Andean compression are exposed in the Chilean side of the Andes. As described in other Andean regions and as verified by physical modelling, magmas can be emplaced under compressive settings migrating horizontally large distances over the flat portion of thrust faults and rising to the surface through the thrust ramps or as in our case using the backthrusts as conduits. The presence of melt in the fault system may have enhanced further deformation and thus the Carrizalito thrust breaks through to the surface thrusting pre-Jurassic and Mesozoic rocks over Cenozoic ones, which produced the uplift of the southern Cordillera Frontal probably in the Late Miocene. In the southern region the Carrizalito thrust remains as a blind thrust, with evidences of modern seismicity suggesting a plausible reactivation of this fault system. The differential uplift along the strike produced by the Carrizalito thrust took place by means of an ENE trending oblique fault, recognized from field data and N-S seismic lines. Thick-skinned structures in the eastern sector were covered discordantly by horizontal basalts of ~0.5 Ma. A shortening of 4.3 km between 10.8 and 0.5 Ma results in a shortening rate of 0.42 mm/a, which indicates that Andean contraction diminished during Late Miocene-Pleistocene times. Some fracture sets in basement rocks support a compression from the WSW.

Overall, our results agree well with most of the regional models of plate tectonics dynamics and GPS geodesy which postulate an ~E-W and fast convergence rate between the Nazca and South American plate from 20 to 11 Ma, and a slightly oblique and slower velocity of convergence from 11 Ma to the present. This suggests that the structural development in the Andean backarc is strongly dependent on the convergence rate of the major plates, however we don´t ruled out changes in the geometry of the subducted slab as responsible of such structural configuration, although available data are not conclusive.

Acknowledgments

The present work forms part of the doctoral studies carried out by the first author (M. Turienzo) and it was financed by several grants from CONICET (PIP 1074), ANPCyT (Picto 841) and SeCyT-UNS (PGI 24/H91). Seismic and well information are gratefully acknowledged to Petroquímica Comodoro Rivadavia and Repsol-YPF. M. Turienzo thanks J. Weber (Grand Valley State University, USA) for providing the plate motion calculations tools. We kindly thank A. Combina (Universidad Nacional de La Rioja), R. Charrier and M. Farías (Universidad de Chile) for their constructive reviews.

References

Alvarado, P.; Beck, S.; Zandt, G.; Araujo, M.; Triep, E. 2005. Crustal deformation in the south central Andes back-arc terranes as viewed from regional broadband seismic waveform modeling. Geophysical Journal International 163: 580-598.

Amrouch, K.; Lacombe, O.; Bellahsen, N., Daniel, J.; Callot, J. 2010. Stress and strain patterns, kinematics and deformation mechanisms in a basement-cored anticline: Sheep Mountain Anticline, Wyoming. Tectonics 29, TC1005. doi: 10.1029/2009TC002525.

Armijo, R.; Rauld, R.; Thiele, R.; Vargas, G.; Campos, J.; Lacassin, R.; Kausel, E. 2010. The West Andean Thrust, the San Ramón Fault, and the seismic hazard for Santiago, Chile. Tectonics 29, TC2007. doi: 10.1029/2008TC002427.

Astini, R.; Dávila, F. 2010. Comment on "The West Andean Thrust, the San Ramón Fault, and the seismic hazard for Santiago, Chile". Tectonics 29, TC4009. doi: 10.1029/2009TC002647.

Baldauf, P. 1997. Timing of the uplift of the Cordillera Principal, Mendoza province, Argentina. Ph.D. Thesis (Unpublished), The George Washington University: 356 p.

Baldauf, P.; Stephens, G.; Kunk, M.; Nullo, F. 1992. Argon-Argon ages for the Huincán intrusive suite and their implications for the structural development of the Andean Foreland, Southern Mendoza province, Argentina. Geological Society of America, Abstracts with Program A-24.

Barazangi, M.; Isacks, B. 1976. Spatial distribution of earthquakes and subduction of the Nazca plate beneath South America. Geology 4: 686-692.

Baker, S.; Gosse, J.; McDonald, E.; Evenson, E.; Martínez, O. 2009. Quaternary history of the piedmont reach of Río Diamante, Argentina. Journal of South American Earth Sciences 28: 54-73.

Bechis, F.; Giambiagi, L.; García, V.; Lanés, S.; Cristallini, E.; Tunik, M. 2010. Kinematic analysis of a transtensional fault system: the Atuel depocenter of the Neuquén Basin, Southern Central Andes, Argentina. Journal of Structural Geology 32 (7): 886-899.

Broens, S.; Pereira, M. 2005. Evolución estructural de la zona de transición entre las fajas plegadas y corridas de Aconcagua y Malargüe Provincia de Mendoza. Revista de la Asociación Geológica Argentina 60 (4): 685-695.

Cahill, T.; Isacks, B. 1992. Seismicity and shape of the subducted Nazca plate. Journal of Geophysical Research 97: 17503-17529.

Caminos, R. 1979. Cordillera Frontal. *In* Segundo Simposio de Geología Regional Argentina, Academia Nacional de Ciencias 1: 397-454, Córdoba, Argentina.

Cardozo, N.; Allmendinger, R.; Morgan, J. 2005. Influence of mechanical stratigraphy and initial stress state on the formation of two fault propagation folds. Journal of Structural Geology 27: 1954-1972.

Charrier, R. 1979. El triásico en Chile y regiones adyacentes de Argentina: una reconstrucción paleogeográfica y paleoclimática. Universidad de Chile, Comunicaciones 26: 1-137.

Charrier, R.; Vicente, J.C. 1972. Liminary and geosynclines Andes; Major orogenic phases and synchronical evolution of the central and austral sectors of the Southern Andes. Conferencia sobre problemas de la tierra sólida 2: 451-470. Buenos Aires.

Charrier, R.; Wyss, A.; Flynn, J.; Swisher, C.; Norell, M.; Zapatta, F.; McKenna, M.; Novaceck, M. 1996. New evidence for late Mesozoic - early Cenozoic evolution of the Chilean Andes in the upper Tinguiririca valley (35°S). Central Chile. Journal of South American Earth Sciences 9 (2): 1-30.

Charrier, R., Baeza, O.; Elgueta, S.; Flynn, J.; Gans, P.; Kay, S.; Muñoz, N.; Wyss, A.; Zurita, E. 2002.

Evidence for Cenozoic extensional basin development and tectonic inversion south of the flat-slab segment, southern central Andes, Chile (33°-36°S.L.). Journal of South American Earth Sciences 15: 117-139.

Combina, A.; Nullo, F.; Stephens, G. 1993. Depósitos Terciarios en el pié de sierra del área de Las Aucas, sur de Mendoza. *In* Congreso Geológico Argentino, No. 12 y Congreso de Exploración de Hidrocarburos, No. 2, Actas 2: 180-186. Mendoza.

Combina, A.; Nullo, F. 1997. Consideraciones tectosedimentarias sobre la Formación Río Diamante, Cordillera de los Andes, Argentina. Cuadernos de Geología Ibérica 22: 305-320. Madrid.

Combina, A.; Nullo, F. 2000. La Formación Loma Fiera (Mioceno superior) y su relación con el volcanismo y el tectonismo neógeno, Mendoza. Revista de la Asociación Geológica Argentina 55 (3): 201-210.

Combina, A.; Nullo, F. 2005. Tertiary volcanism and sedimentation in the southern Cordillera Principal, Mendoza, Argentina. *In* International Symposium on Andean Geodinamics, No. 6: 174-177. Barcelona.

Combina, A.; Nullo, F. 2008. El "diacronismo" de la Formación Agua de la Piedra (Terciario, Mendoza). *In* Congreso Geológico Argentino, No. 17, Actas 1: 87-88. Jujuy.

Combina, A.; Nullo, F. 2011. Ciclos tectónicos, volcánicos y sedimentarios del Cenozoico del sur de Mendoza-Argentina (35°-37°S y 69°30'W). Andean Geology 38 (1): 198-218.

Cortés, J.; Vinciguerra, P.; Yamín, M.; Pasini, M. 1999. Tectónica cuaternaria de la región Andina del Nuevo Cuyo (28º - 38ºLS). *In* Geología Argentina (Caminos, R.; editor). Instituto de Geología y Recursos Minerales, Anales 29 (24): 760-778. Buenos Aires.

Cristallini, E. 2005. Modelos cinemático-numéricos de pliegues relacionados a fallas. *In* Congreso Geológico Argentino, No. 16, Actas 1: 425-426. La Plata.

Cruz, C. 1993. Facies y estratigrafía secuencial del Cretácico superior en la zona del río Diamante, Provincia de Mendoza, Argentina. *In* Congreso Geológico Argentino, No. 12 y Congreso de Exploración de Hidrocarburos, No. 2, Actas 1: 46-54. Mendoza.

Davis, D.; Suppe, J.; Dahlen, F. 1983. Mechanics of fold-and-thrust belts and accretionary wedges. Journal of Geophysical Research 88: 1153-1172.

Deckart, K.; Godoy, E.; Bertens, A.; Jerez, D.; Saeed, A. 2010. Barren Miocene granitoids in the Central Andean metallogenic belt, Chile: Geochemistry and Nd-Hf and U-Pb isotope systematics Andean Geology 37 (1): 1-31.

Dessanti, R.; Caminos, R. 1967. Edades Potasio-Argón y posición estratigráfica de algunas rocas ígneas y metamórficas de la Precordillera, Cordillera Frontal y Sierras de San Rafael, provincia de Mendoza. Revista de la Asociación Geológica Argentina 22 (2): 135-162.

Dewey, J. F.; Bird, J.M. 1970. Mountain belts and the new global tectonics. Journal of Geophysical Research 75: 2625-2647.

Dimieri, L. 1992a. Evolución estructural de la Cordillera Principal, a lo largo del arroyo La Vaina, entre el arroyo Potimalal y el arroyo Pehuenche, al oeste de Bardas Blancas, Mendoza. Ph.D. Thesis (Unpublished), Universidad Nacional del Sur: 151 p.

Dimieri, L. 1992b. Emplazamiento lacolítico a través de retrocorrimientos, cerro Palao Mahuida, Bardas Blancas, Mendoza. Academia Nacional de Ciencias Exactas, Físicas y Naturales, Monografías 8: 163-166.

Erslev, E., Holdaway, S.; O'Meara, S.; Jurista, B.; Selvig, B. 2004. Laramide minor faulting in the Colorado Front Range. New Mexico Bureau of Geology and Mineral Resources 160: 181-203.

Farías, M.; Charrier, R.; Carretier, S.; Martinod, J.; Fock, A.; Campbell, D.; Cáceres, J.; Comte, D. 2008. Late Miocene high and rapid surface uplift and its erosional response in the Andes of central Chile (33°-35°S). Tectonics 27: TC1005. doi: 10.1029/2006TC002046.

Farías, M.; Comte, D.; Charrier, R.; Martinod, J.; David, C.; Tassara, A.; Tapia, F.; Fock, A. 2010. Crustal-scale structural architecture in central Chile based on seismicity and surface geology: Implications for Andean mountain building. Tectonics 29: TC3006. doi: 10.1029/2009TC002480.

Fortunatti, N. 2009. Evolución Estructural Andina para el Valle del Río Atuel entre el Cerro Sosneado y la Cuchilla de la Tristeza, Provincia de Mendoza, Argentina. Ph.D. Thesis (Unpublished), Universidad Nacional del Sur: 168 p.

Franzese, J.; Spalletti, L. 2001. Late Triassic-Early Jurassic continental extension in southwestern Gondwana: tectonic segmentation and pre-break-up rifting. Journal of South American Earth Sciences 14: 257-270.

Fuentes, F.; Ramos, V. 2008. Geología de la región del cerro Guanaquero, río Diamante, Mendoza. Revista de la Asociación Geológica Argentina 63 (1): 84-96.

Galarza, B.; Zamora Valcarce, G.; Folguera, A.; Bottesi, G. 2009. Geología y evolución tectónica del frente cordillerano a los 36º30'S: bloques de Yihuinhuaca y Puntilla de Huincán. Mendoza. Revista de la Asociación Geológica Argentina 65 (1): 170-191.

Galland, O.; Hallot, E.; Cobbold, P.; Ruffet, G.; Bremond d'Ars, J. 2007a. Volcanism in a compressional Andean setting: A structural and geochronological study of Tromen Volcano (Neuquén province, Argentina). Tectonics 26: TC4010. doi: 10.1029/2006TC002011.

Galland, O.; Cobbold, P.; Bremond d'Ars, J.; Hallot, E. 2007b. Rise and emplacement of magma during horizontal shortening of the brittle crust: Insights from experimental modeling. Journal of Geophysical Research 112: B06402. doi: 10.1029/2006JB004604.

García, P.; Davis, G. 2004. Evidence and mechanisms for folding of granite, Sierra de Hualfín basement-cored uplift, northwest Argentina. American Association of Petroleum Geologists Bulletin 88: 1255-1276.

Gerth, E. 1931. La estructura geológica de la Cordillera Argentina entre el río Grande y el río Diamante en el sud de la provincia de Mendoza. Academia Nacional de Ciencias 10: 123-174. Cordoba.

Giambiagi, L.; Ramos, V. 2002. Structural evolution of the Andes between 33°30' and 33°45'S, above the transition zone between the flat and normal subduction segment, Argentina and Chile. Journal of South American Earth Sciences 15: 101-116.

Giambiagi, L.; Ramos, V.; Godoy, E.; Álvarez, P.; Orts, S. 2003. Cenozoic deformation and tectonic style of the Andes, between 33° and 34° South Latitude. Tectonics 22: 1041. doi: 10.1029/2001TC001354.

Giambiagi, L.; Álvarez, P.; Bechis, F.; Tunik, M. 2005a. Influencia de las estructuras de rift triásico-jurásicas sobre el estilo de deformación en las fajas plegadas y corridas de Aconcagua y Malargüe, Mendoza. Revista de la Asociación Geológica Argentina 60 (4): 662-671.

Giambiagi, L.; Suriano, J.; Mescua, J. 2005b. Extensión multiepisódica durante el Jurásico temprano en el depocentro Atuel de la cuenca Neuquina. Revista de la Asociación Geológica Argentina 60 (3): 524-534.

Giambiagi, L.; Bechis, F.; García, V.; Clark, A. 2008. Temporal and spatial relationships of thick- and thin-skinned deformation: A case study from the Malargüe fold-and-thrust belt, southern Central Andes. Tectonophysics 459: 123-139.

Giambiagi, L.; Ghiglione, M.; Cristallini, E.; Bottesi, G. 2009. Kinematic models of basement/cover interaction: Insights from the Malargüe fold and thrust belt, Mendoza, Argentina. Journal of Structural Geology 31: 1443-1457.

Godoy, E.; Yáñez, G.; Vera, E. 1999. Inversion of an Oligocene volcano-tectonic basin and uplift of its superimposed Miocene magmatic arc, Chilean central Andes: First seismic and gravity evidence. Tectonophysics 306: 217-236.

González, G.; Cembrano, J.; Aron, F.; Veloso, E.; Shyu, J. 2009. Coeval compressional deformation and volcanism in the central Andes, case studies from northern Chile (23°S-24°S). Tectonics 28: TC6003. doi. 10.1029/2009TC002538.

Groeber, P. 1947. Observaciones geológicas a lo largo del meridiano70, 2: Hojas Sosneao y Maipo. Revista de la Asociación Geológica Argentina 2 (2): 141-176.

Gulisano, C.; Gutiérrez Pleimling, A. 1994. Field Guide: The Jurassic of the Neuquén Basin, b) Mendoza Province. Asociación Geológica Argentina, serie E 3: 103 p. Buenos Aires.

Hancock, P. 1985. Brittle microtectonics: principles and practice. Journal of Structural Geology 7: 437-457.

Heermance, R.; Chen, J.; Burbank, D.; Miao, J. 2008. Temporal constraints and pulsed Late Cenozoic deformation during the structural disruption of the active Kashi foreland, northwest China. Tectonics 27: TC6012. doi: 10.1029-72007TC002226.

Hervé, F.; Davison, J.; Godoy, E.; Mpodozis, C.; Covacevich, V. 1981. The Late Paleozoic in Chile; Stratigraphy, structure, and possible tectonic framework. Anais da Academia Brasileira de Ciencias 53: 361-373.

Hollister, L.; Crawford, M. 1986. Melt-enhanced deformation: A major tectonic process. Geology 14: 558-561.

James, D. 1971. Plate tectonic model for the evolution of the Central Andes. Geological Society of America Bulletin 82: 3325-3346.

Jordan, T.; Isacks, B.; Allmendinger, R.; Brewer, J.; Ramos, V.; Ando, C. 1983. Andean tectonics related to geometry of subducted Nazca plate. Geological Society of America Bulletin 94: 341-361.

Kay, S.; Burns, W.; Copeland, P.; Mancilla, O. 2006. Late Cretaceous to Recent magmatism over the Neuquén basin: Evidence for transient shallowing of the subduction zone under the Neuquén Andes (36°S to 38°S latitude). *In* Evolution of an Andean margin: A tectonic and magmatic view from the Andes to the Neuquén Basin (35°-39°S lat) (Kay, S.; Ramos, V.; editors). Geological Society of America Special Paper 407: 19-60.

Kendrick, E.; Bevis, M.; Smalley, R.; Brooks, B.; Barriga Vargas, R.; Lauría, E.; Souto Fortes, L. 2003. The Nazca-South America Euler vector and its rate of change. Journal of South American Earth Sciences 16: 125-131.

Kendrick, E.; Brooks, B.; Bevis, M.; Smalley, R.; Lauría, E.; Araujo, M.; Parra, H. 2006. Active orogeny of

the South-Central Andes studied with GPS geodesy. Revista de la Asociación Geológica Argentina 61 (4): 555-566.

Kim, H.; Scaricabarozzi, N.; Ramos, V. 2005. La estructura al sur del río Diamante y su relación con la falla de Malargüe, Cuenca Neuquina, centro-oeste de Mendoza. *In* Congreso Geológico Argentino, No. 16, Actas 2: 63-70. La Plata.

Kley, J. 1996. Transition from basement-involved to thin-skinned thrusting in the Cordillera Oriental of southern Bolivia. Tectonics 15: 763-775.

Knipe, R. 1990. Microstructural analysis and tectonic evolution in thrust systems: examples from the Assynt region of the Moine Thrust zone, Scotland. *In* Deformation Mechanisms in Ceramics, Minerals and Rocks (Barber, D.J.; Meredith, P.G.; editors). Mineralogical Society of Great Britain and Ireland, Unwin Hyman: 228-261. London

Kozlowski, E. 1984. Interpretación estructural de la Cuchilla de la Tristeza. Provincia de Mendoza. *In* Congreso Geológico Argentino, No. 11, Actas 2: 381-395. Bariloche.

Kozlowski, E.; Cruz, C; Sylwan, C. 1996. Geología estructural de la zona de Chos Malal, Cuenca Neuquina, Argentina. *In* Congreso Geológico Argentino, No. 13, Actas 1: 15-26. Buenos Aires.

Lanés, S. 2005. Late Triassic to Early Jurassic sedimentation in northern Neuquén Basin, Argentina: Tectosedimentary Evolution of the First Transgression. Geologica Acta 3: 81-106.

Lanés, S.; Giambiagi, L.; Bechis, F.; Tunik, M. 2008. Late Triassic-Early Jurassic successions of the Atuel depocenter: sequence stratigraphy and tectonic controls. Revista de la Asociación Geológica Argentina 63 (4): 534-548.

Legarreta, L.; Gulisano, C. 1989. Análisis estratigráfico secuencial de la Cuenca Neuquina (Triásico superior-Terciario inferior). *In* Cuencas Sedimentarias Argentinas (Chebli, G.; Spalletti, L.; editors). Correlación Geológica Serie 6: 221-243.

Legarreta, L.; Uliana, M. 1991. Jurassic-Cretaceous marine oscillations and geometry of back-arc basin fill, central Argentine Andes. *In* Sedimentation, Tectonics and Eustasy: Sea level Changes at Active Plate Margins (MacDonald, D.; editor). International Association of Sedimentologists, Special Publication 12: 429-450, Oxford.

Likerman, J.; Cristallini, E.; Selles Martínez, J. 2011. Estudio de fracturas asociado al sistema de plegamiento den la localidad de Tres Cruces, Provincia de Jujuy. *In* Congreso Geológico Argentino, No. 18, Actas DVD, S12: 790-791. Neuquén.

Llambías, E.; Kleiman, L.; Salvarredi, J. 1993. El Magmatismo Gondwánico. *In* Geología y Recursos Naturales de Mendoza (Ramos, V.; editor). Congreso Geológico Argentino, No. 12 y Congreso de Exploración de Hidrocarburos, No. 2, Relatorio: 53-64.

Maksaev, V.; Zentilli, M.; Munizaga, F.; Charrier, R. 2003. Denudación/alzamiento del Mioceno superior- Plioceno inferior de la Cordillera de Chile central (33º-35ºS) inferida por dataciones por trazas de fisión en apatito de plutones miocenos. *In* Congreso Geológico Chileno, No. 10, Simposio 1, Actas en CD. Concepción.

Manceda, R.; Figueroa, D. 1995. Inversion of the Mesozoic Neuquén Rift in the Malargüe Fold and Thrust Belt, Mendoza, Argentina. *In* Petroleum basins of South America (Tankard, A.; Suárez R.; Welsink, H.; editors). American Association of Petroleum Geologists, Memoir 62: 369-382.

Manceda, R.; Bollatti, N.; Manoti, R. 1992. Modelo estructural para Bardas Blancas, cuenca Neuquina, Mendoza. Boletín de Informaciones Petroleras 9 (31): 92-103.

McQuarrie, N.; Barnes, J.; Ehlers, T. 2008. Geometric, kinematic, and erosional history of the central Andean Plateau, Bolivia (15-17°S). Tectonics 27: TC3007. doi: 10.1029/2006TC002054.

Mescua, J.; Giambiagi, L.; Bechis, F. 2008. Evidencias de tectónica extensional en el Jurásico tardío (Kimeridgiano) del suroeste de la provincia de Mendoza. Revista de la Asociación Geológica Argentina 63 (4): 512-519.

Mescua, J.; Giambiagi, L.; Ramos, V. 2010. Inherited controls in Andean structure in a sector of the Malargüe fold-and-thrust belt, Mendoza province, Argentina. Trabajos de Geología, Universidad de Oviedo 30: 81-86.

Norabuena, E.; Dixon, T.; Stein, S.; Harrison, C. 1999. Decelerating Nazca-South America and Nazca-Pacific plate motions. Geophysical Research Letters 26: 3405-3408.

Nullo, F.; Stephens, G.; Otamendi, J.; Baldauf, P. 2002. El volcanismo del Terciario superior del sur de Mendoza. Revista de la Asociación Geológica Argentina 57 (2): 119-132.

Orts, S.; Ramos, V. 2006. Evidence of middle to late cretaceous compressive deformation in the High Andes of Mendoza, Argentina. Geological Society of America Special Meeting and Asociación Geológica Argentina Special Publication 9: 65. Mendoza.

Pardo-Casas, F.; Molnar, P. 1987. Relative motion of the Nazca (Farallon) and South American plates since Late Cretaceous time. Tectonics 6: 233-248.

Pinto, L.; Muñoz, C.; Nalpas, T.; Charrier, R. 2010. Role of sedimentation during basin inversion in analogue modeling. Journal of Structural Geology 32: 554-565.

Piquer, J.; Castelli, J.; Charrier, R.; Yáñez, G. 2010. El Cenozoico del alto río Teno, Cordillera Principal, Chile central: estratigrafía, plutonismo y su relación con estructuras profundas. Andean Geology 37 (1): 32-53.

Polanski, J. 1963. Estratigrafía, Neotectónica y Geomorfología del Pleistoceno pedemontano de Mendoza. Revista de la Asociación Geológica Argentina 17 (3-4): 181-199.

Ramos, V. 1988. The tectonics of the Central Andes; 30º to 33ºS latitude. *In* Processes in Continental Lithospheric Deformation (Clark, S.; Burchfiel, D.; editors). Geological Society of America Special Paper 218: 31-54.

Ramos, V. 2009. Anatomy and global context of the Andes: Main geological features and the Andean orogenic cycle. *In* Backbone of the Americas: Shallow subduction, Plateau uplift, and Ridge and Terrane collision (Kay, S.; Ramos, V.; Dickinson, W.; editors). Geological Society of America Memoir 204: 31-66.

Ramos, V.; Kay, S. 1991. Triassic rifting and associated basalts in the Cuyo basin, central Argentina. *In* Andean Magmatism and its Tectonic Setting (Harmon, R.; Rapela, C.; editors). Geological Society of America Special Paper 265: 79-91.

Ramos, V.; Folguera, A. 2005. Tectonic evolution of the Andes of Neuquén: constraints derived from the magmatic arc and foreland deformation. *In* The Neuquén Basin: A Case Study in Sequence Stratigraphy and Basin Dynamics (Veiga, G.; Spalletti, L.; Howell, J.; Schwarz, E.; editors). The Geological Society, Special Publication 252: 15-35.

Ramos, V.; Kay, S. 2006. Overview of the tectonic evolution of the southern Central Andes of Mendoza and Neuquén (35°-39°S latitude). *In* Evolution of an Andean margin: A tectonic and magmatic view from the Andes to the Neuquén Basin (35°-39°S lat) (Kay, S.; Ramos, V.; editors). Geological Society of America Special Paper 407: 1-18.

Ramos, V.; Cristallini, E.; Pérez, D. 2002. The Pampean flat-slab of the Central Andes. Journal of South American Earth Sciences 15: 59-78.

Rojas, L.; Radic, P. 2002. Estilos de deformación del basamento y de la cobertura sedimentaria en la faja plegada y fallada de Malargüe en el área de Puesto Rojas, Mendoza, Argentina. *In* Congreso Geológico Argentino, No. 15, Actas 3: 224-229. El Calafate.

Sanz, P.; Pollard, D.; Allwardt, P.; Borja, R. 2008. Mechanical models of fracture reactivation and slip on bedding surfaces during folding of the asymmetric anticline at Sheep Mountain, Wyoming. Journal of Structural Geology 30: 1177-1191.

Schönborn, G. 1999. Balancing cross-sections with kinematic constrains: The Dolomites (northern Italy). Tectonics 18: 527-545.

Silvestro, J.; Kraemer, P.; Achilli, F.; Brinkworth, W. 2005. Evolución de las cuencas sinorogénicas de la Cordillera Principal entre 35°-36°S, Malargüe. Revista de la Asociación Geológica Argentina 60 (4): 627-643.

Silvestro, J.; Atencio, M. 2009. La cuenca cenozoica del río Grande y Palauco: edad, evolución y control estructural, faja plegada de Malargüe. Revista de la Asociación Geológica Argentina 65 (1): 154-169.

Somoza, R. 1998. Updated Nazca (Farallón)-South America relative motions during the last 40 My: implications for mountain building in the central Andean region. Journal of South American Earth Sciences 11: 211-215.

Spalletti, L. 1999. Cuencas triásicas del oeste argentino: origen y evolución. Acta Geológica Hispánica 32: 29-50.

Spalletti, L.; Franzese, J.; Morel, E.; Artabe, A. 2005. Nuevo enfoque estratigráfico del Triásico-Jurásico temprano en la región del Río Atuel, provincia de Mendoza. *In* Congreso Geológico Argentino, No. 16, Actas 3: 77-82. La Plata.

Sruoga, P.; Etcheverría, M.; Folguera, A.; Repol, D. 2005. Hoja Geológica 3569-I, Volcán Maipo, Provincia de Mendoza. SEGEMAR, 290: 114 p. Buenos Aires.

Suppe, J.; Connors, C.; Zhang, Y. 2004. Shear fault-bend folding. *In* Thrust tectonics and hydrocarbon systems (McClay, K.; editor). American Association of Petroleum Geologists Memoir 82: 303-323.

Tibaldi, A. 2005. Volcanism in compressional tectonic settings: Is it possible?. Geophysical Research Letters 32: L06309. doi: 10.1029/2004GL0217098.

Tickyj, H.; Rodríguez Raising, M.; Cingolani, C.; Alfaro, M.; Uriz, N. 2009.Graptolitos Ordovícicos en el sur de la Cordillera Frontal de Mendoza, Argentina. Revista de la Asociación Geológica Argentina 64 (2): 295-302.

Torres Carbonell, P.; Dimieri, L. 2011. Mecanismo de acortamiento de basamento y cobertura en los Andes Fueguinos. *In* Congreso Geológico Argentino, No. 18, Actas DVD, S12: 877-878. Neuquén.

Tunik, M.; Aguirre Urreta, B.; Concheyro, A. 2005. El Grupo Mendoza a la latitud del Río Diamante, cuenca Neuquina Surmendocina. *In* Congreso Geológico Argentino, No. 16, Actas 1: 325-330.

Tunik, M.; Folguera, A.; Naipauer, M.; Pimentel, M.; Ramos, V. 2010. Early uplift and orogenic deformation in the neuquén basin: constraints on the Andean uplift

from U-Pb and Hf isotopic data of detrital zircons. Tectonophysics 489 (1-4): 258-273.

Turienzo, M. 2008. Estructuras tectónicas en el frente montañoso de la Cordillera Principal, a lo largo del Río Diamante (34°40' L.S. - 69°30' L.O), provincia de Mendoza. Ph.D. Thesis (Unpublished), Universidad Nacional del Sur: 254 p.

Turienzo, M. 2010. Structural style of the Malargüe fold-and-thrust belt at the Diamante River area (34º30' - 34º50' S) and its linkage with the Cordillera Frontal, Andes of central Argentina. Journal of South American Earth Sciences 29: 537-556.

Turienzo, M.; Dimieri, L. 2005a. Geometría y cinemática de las estructuras que involucran al basamento en la zona del arroyo Tordillo, faja corrida y plegada de Malargüe, Mendoza. Revista de la Asociación Geológica Argentina 64 (4): 651-661.

Turienzo, M.; Dimieri, L. 2005b. Interpretación de la estructura del frente montañoso en la zona del Río Diamante, Mendoza. Revista de la Asociación Geológica Argentina 60 (2): 336-352.

Turienzo, M.; Dimieri, L. 2005c. Geometric and kinematic model for basement-involved backthrusting at Diamante River, southern Andes, Mendoza province, Argentina. Journal of South American Earth Sciences 19: 111-125.

Turienzo, M.; Dimieri, L. 2006. Cinemática de los sistemas de retrocorrimiento que afectan al basamento, Río Diamante, Mendoza. Asociación Geológica Argentina, Publicación Especial 9: 142-148.

Turienzo, M.; Frisicale, C.; Torres Carbonell, P.; Dimieri, L. 2006. Micro y meso estructuras andinas en el basamento de la faja corrida y plegada de Malargüe, Río Diamante, Mendoza. Asociación Geológica Argentina, Publicación Especial 9: 221-228.

Twiss, R.; Moores, E. 2007. Structural Geology. W.H. Freeman and Company: 736 p. USA.

Uliana, M.; Biddle, K.; Cerdán, J. 1989. Mesozoic extension and the formation of Argentine sedimentary basins. *In* Extensional Tectonics and Stratigraphy of the North Atlantic Margins (Tankard, A.; Balkwill, H.; editors). American Association of Petroleum Geologists, Memoir 46: 599-614.

Volkheimer, W. 1978. Descripción geológica de la hoja 27b, Cerro Sosneado, Provincia de Mendoza. SEGEMAR, 151: 85 p. Buenos Aires.

Wibberley, C. 1997. Three-dimensional geometry, strain rates and basement deformation mechanisms of thrust-bend folding. Journal of Structural Geology 19: 535-550.

Williams, G.; Powell, C; Cooper, M. 1989. Geometry and kinematics of inversion tectonics. *In* Inversion Tectonics (Cooper, M.; Williams, G.; editors). Geological Society of London, Special Publication 44: 3-15.

Yagupsky, D.; Cristallini, E.; Fantín, J.; Zamora Valcarce, G.; Bottesi, G.; Varadé, R. 2008. Oblique half-graben inversion of the Mesozoic Neuquén Rift in the Malargüe Fold and Thrust Belt, Mendoza, Argentina: New insights from analogue models. Journal of Structural Geology 30: 839-853.

Yrigoyen, M. 1993. Los depósitos sinorogénicos terciarios. *In* Geología y Recursos Naturales de Mendoza (Ramos, V.; editor). Congreso Geológico Argentino, No. 12 y Congreso de Exploración de Hidrocarburos, No. 2, Relatorio: 123-148.

Zapata, T.; Dzelalija, F.; Olivieri, G. 2001. Desarrollo de reservorios fracturados de la Formación Mulichinco usando modelado estructural 3D: yacimiento Filo Morado, Cuenca Neuquina, Argentina. Boletín de Informaciones Petroleras 3 (18): 38-47.

Manuscript received: March 31, 2011; revised/accepted: October 28, 2011; available online: November 17, 2011.